EXHIBIT A

Nucleotide

Display Settings: GenBank

Showing 1.35kb region from base 2459322 to 2460668.

Escherichia coli str. K-12 substr. MG1655, complete genome

GenBank: U00096.2

FASTA Graphics

```
LOCUS       U00096                 1347 bp    DNA     linear   BCT 25-OCT-2010
DEFINITION  Escherichia coli str. K-12 substr. MG1655, complete genome.
ACCESSION   U00096 REGION: 2459322..2460668
VERSION     U00096.2  GI:48994873
DBLINK      Project: 225
KEYWORDS    .
SOURCE      Escherichia coli str. K-12 substr. MG1655
  ORGANISM  Escherichia coli str. K-12 substr. MG1655
            Bacteria; Proteobacteria; Gammaproteobacteria; Enterobacteriales;
            Enterobacteriaceae; Escherichia.
REFERENCE   1  (bases 1 to 1347)
  AUTHORS   Blattner,F.R., Plunkett,G. III, Bloch,C.A., Perna,N.T., Burland,V.,
            Riley,M., Collado-Vides,J., Glasner,J.D., Rode,C.K., Mayhew,G.F.,
            Gregor,J., Davis,N.W., Kirkpatrick,H.A., Goeden,M.A., Rose,D.J.,
            Mau,B. and Shao,Y.
  TITLE     The complete genome sequence of Escherichia coli K-12
  JOURNAL   Science 277 (5331), 1453-1474 (1997)
   PUBMED   9278503
REFERENCE   2  (bases 1 to 1347)
  AUTHORS   Riley,M., Abe,T., Arnaud,M.B., Berlyn,M.K., Blattner,F.R.,
            Chaudhuri,R.R., Glasner,J.D., Horiuchi,T., Keseler,I.M., Kosuge,T.,
            Mori,H., Perna,N.T., Plunkett,G. III, Rudd,K.E., Serres,M.H.,
            Thomas,G.H., Thomson,N.R., Wishart,D. and Wanner,B.L.
  TITLE     Escherichia coli K-12: a cooperatively developed annotation
            snapshot--2005
  JOURNAL   Nucleic Acids Res. 34 (1), 1-9 (2006)
   PUBMED   16397293
  REMARK    Publication Status: Online-Only
REFERENCE   3  (bases 1 to 1347)
  AUTHORS   Arnaud,M., Berlyn,M.K.B., Blattner,F.R., Galperin,M.Y.,
            Glasner,J.D., Horiuchi,T., Kosuge,T., Mori,H., Perna,N.T.,
            Plunkett,G. III, Riley,M., Rudd,K.E., Serres,M.H., Thomas,G.H. and
            Wanner,B.L.
  TITLE     Workshop on Annotation of Escherichia coli K-12
  JOURNAL   Unpublished
  REMARK    Woods Hole, Mass., on 14-18 November 2003 (sequence corrections)
REFERENCE   4  (bases 1 to 1347)
  AUTHORS   Glasner,J.D., Perna,N.T., Plunkett,G. III, Anderson,B.D.,
            Bockhorst,J., Hu,J.C., Riley,M., Rudd,K.E. and Serres,M.H.
  TITLE     ASAP: Escherichia coli K-12 strain MG1655 version m56
  JOURNAL   Unpublished
  REMARK    ASAP download 10 June 2004 (annotation updates)
REFERENCE   5  (bases 1 to 1347)
  AUTHORS   Hayashi,K., Morooka,N., Mori,H. and Horiuchi,T.
  TITLE     A more accurate sequence comparison between genomes of Escherichia
            coli K12 W3110 and MG1655 strains
  JOURNAL   Unpublished
  REMARK    GenBank accessions AG613214 to AG613378 (sequence corrections)
REFERENCE   6  (bases 1 to 1347)
  AUTHORS   Perna,N.T.
  TITLE     Escherichia coli K-12 MG1655 yqiK-rfaE intergenic region, genomic
            sequence correction
  JOURNAL   Unpublished
  REMARK    GenBank accession AY605712 (sequence corrections)
REFERENCE   7  (bases 1 to 1347)
  AUTHORS   Rudd,K.E.
  TITLE     A manual approach to accurate translation start site annotation: an
            E. coli K-12 case study
  JOURNAL   Unpublished
REFERENCE   8  (bases 1 to 1347)
  AUTHORS   Blattner,F.R. and Plunkett,G. III.
  TITLE     Direct Submission
  JOURNAL   Submitted (16-JAN-1997) Laboratory of Genetics, University of
            Wisconsin, 425G Henry Mall, Madison, WI 53706-1580, USA
REFERENCE   9  (bases 1 to 1347)
  AUTHORS   Blattner,F.R. and Plunkett,G. III.
  TITLE     Direct Submission
  JOURNAL   Submitted (02-SEP-1997) Laboratory of Genetics, University of
            Wisconsin, 425G Henry Mall, Madison, WI 53706-1580, USA
REFERENCE   10 (bases 1 to 1347)
  AUTHORS   Plunkett,G. III.
  TITLE     Direct Submission
  JOURNAL   Submitted (13-OCT-1998) Laboratory of Genetics, University of
            Wisconsin, 425G Henry Mall, Madison, WI 53706-1580, USA
REFERENCE   11 (bases 1 to 1347)
  AUTHORS   Plunkett,G. III.
  TITLE     Direct Submission
  JOURNAL   Submitted (10-JUN-2004) Laboratory of Genetics, University of
            Wisconsin, 425G Henry Mall, Madison, WI 53706-1580, USA
  REMARK    Sequence update by submitter
REFERENCE   12 (bases 1 to 1347)
  AUTHORS   Plunkett,G. III.
  TITLE     Direct Submission
  JOURNAL   Submitted (07-FEB-2006) Laboratory of Genetics, University of
            Wisconsin, 425G Henry Mall, Madison, WI 53706-1580, USA
  REMARK    Protein updates by submitter
REFERENCE   13 (bases 1 to 1347)
  AUTHORS   Rudd,K.E.
  TITLE     Direct Submission
  JOURNAL   Submitted (24-APR-2007) Department of Biochemistry and Molecular
            Biology, University of Miami Miller School of Medicine, 118 Gautier
```

Bldg., Miami, FL 33136, USA
REMARK Annotation update from ecogene.org as a multi-database collaboration
REFERENCE 14 (bases 1 to 1347)
AUTHORS Rudd,K.E.
TITLE Direct Submission
JOURNAL Submitted (20-SEP-2010) Department of Biochemistry and Molecular Biology, University of Miami Miller School of Medicine, 118 Gautier Bldg., Miami, FL 33136, USA
REMARK Annotation update from ecogene.org as a multi-database collaboration
COMMENT On or before Jun 21, 2004 this sequence version replaced gi:1786181, gi:1786192, gi:2367095, gi:1786217, gi:1786230, gi:1786240, gi:1786250, gi:1786262, gi:1786281, gi:1786298, gi:1786306, gi:1786316, gi:1786327, gi:1786339, gi:1786348, gi:1786358, gi:1786370, gi:1786383, gi:1786389, gi:1786402, gi:1786415, gi:2367098, gi:2367099, gi:1786454, gi:1786465, gi:2367102, gi:2367103, gi:1786501, gi:1786510, gi:1786530, gi:1786532, gi:1786542, gi:1786554, gi:1786568, gi:1786590, gi:1786596, gi:1786603, gi:1786614, gi:1786628, gi:1786639, gi:1786649, gi:1786660, gi:1786671, gi:1786683, gi:1786692, gi:1786705, gi:1786716, gi:1786728, gi:1786739, gi:1786751, gi:1786766, gi:1786782, gi:1786790, gi:1786800, gi:1786808, gi:1786819, gi:1786836, gi:1786849, gi:1786862, gi:1786875, gi:1786888, gi:1786896, gi:1786910, gi:1786920, gi:1786934, gi:1786947, gi:1786955, gi:1786967, gi:1786978, gi:1786988, gi:1786998, gi:1787015, gi:1787025, gi:1787036, gi:1787047, gi:1787058, gi:1787070, gi:1787084, gi:1787097, gi:1787106, gi:1787115, gi:1787125, gi:1787134, gi:1787148, gi:1787156, gi:1787169, gi:1787180, gi:1787189, gi:1787202, gi:2367111, gi:2367113, gi:1787233, gi:1787248, gi:1787256, gi:1787265, gi:1787282, gi:1787293, gi:1787308, gi:1787332, gi:1787337, gi:1787345, gi:1787358, gi:1787371, gi:1787382, gi:1787405, gi:1787417, gi:1787434, gi:1787444, gi:1787453, gi:1787467, gi:1787476, gi:1787486, gi:1787496, gi:1787509, gi:1787523, gi:2367115, gi:1787543, gi:2367117, gi:1787566, gi:1787578, gi:1787586, gi:1787600, gi:1787613, gi:1787631, gi:1787642, gi:1787652, gi:1787665, gi:1787673, gi:1787682, gi:1787695, gi:1787706, gi:1787720, gi:1787730, gi:1787742, gi:1787752, gi:1787764, gi:1787773, gi:1787783, gi:1787790, gi:1787801, gi:1787814, gi:2367119, gi:1787847, gi:1787862, gi:1787875, gi:1787888, gi:1787898, gi:2367121, gi:1787921, gi:1787935, gi:1787945, gi:1787955, gi:1787966, gi:1787978, gi:2367122, gi:1787997, gi:1788011, gi:1788022, gi:1788033, gi:1788045, gi:1788058, gi:1788067, gi:1788078, gi:1788089, gi:1788106, gi:1788117, gi:1788129, gi:1788139, gi:1788154, gi:1788163, gi:1788179, gi:1788189, gi:1788200, gi:1788214, gi:1788225, gi:1788241, gi:1788257, gi:2367124, gi:1788286, gi:2367125, gi:1788298, gi:1788310, gi:2367127, gi:1788338, gi:1788354, gi:1788373, gi:1788382, gi:1788395, gi:1788413, gi:1788425, gi:2367129, gi:1788447, gi:1788456, gi:1788470, gi:1788479, gi:1788489, gi:1788498, gi:1788508, gi:1788520, gi:2367131, gi:1788547, gi:1788555, gi:2367132, gi:1788570, gi:1788582, gi:1788596, gi:1788605, gi:1788623, gi:1788634, gi:1788647, gi:1788655, gi:1788672, gi:1788684, gi:1788694, gi:1788709, gi:1788718, gi:1788731, gi:2367135, gi:2367137, gi:1788763, gi:1788775, gi:1788789, gi:1788805, gi:1788813, gi:1788821, gi:1788835, gi:1788850, gi:1788862, gi:1788870, gi:1788883, gi:1788899, gi:1788907, gi:2367139, gi:1788927, gi:1788939, gi:2367141, gi:2367142, gi:1788975, gi:2367143, gi:2367147, gi:1789011, gi:1789024, gi:1789037, gi:2367149, gi:2367151, gi:2367153, gi:2367155, gi:2367158, gi:1789110, gi:2367157, gi:2367160, gi:1789147, gi:1789153, gi:2367162, gi:2367163, gi:1789185, gi:1789195, gi:2367165, gi:2367168, gi:2367170, gi:1789239, gi:2367171, gi:2367173, gi:1789270, gi:1789282, gi:2367176, gi:2367178, gi:1789319, gi:2367179, gi:1789344, gi:2367181, gi:2367182, gi:2367184, gi:2367186, gi:1789405, gi:2367187, gi:1789431, gi:1789441, gi:1789451, gi:2367189, gi:2367191, gi:2367194, gi:1789495, gi:2367197, gi:1789524, gi:1789536, gi:2367199, gi:1789562, gi:2367201, gi:2367203, gi:1789607, gi:1789619, gi:2367205, gi:2367207, gi:1789659, gi:2367209, gi:2367211, gi:1789694, gi:1789728, gi:1789734, gi:2367213, gi:1789758, gi:2367215, gi:1789783, gi:1789798, gi:2367219, gi:2367220, gi:2367222, gi:2367227, gi:1789840, gi:1789854, gi:1789868, gi:1789880, gi:2367230, gi:2367232, gi:1789918, gi:1789929, gi:1789931, gi:2367235, gi:2367238, gi:1789957, gi:2367241, gi:1789977, gi:1789989, gi:2367244, gi:2367246, gi:2367249, gi:2367251, gi:1790016, gi:2367252, gi:1790063, gi:2367253, gi:2367255, gi:2367258, gi:1790105, gi:2367261, gi:2367266, gi:1790142, gi:2367269, gi:1790166, gi:2367272, gi:1790188, gi:2367276, gi:2367278, gi:2367282, gi:2367291, gi:2367294, gi:2367299, gi:2367306, gi:2367315, gi:2367318, gi:1790295, gi:2367320, gi:2367324, gi:2367326, gi:2367328, gi:1790356, gi:1790374, gi:1790385, gi:2367332, gi:1790404, gi:2367333, gi:2367336, gi:1790440, gi:1790448, gi:1790456, gi:2367338, gi:2367339, gi:2367340, gi:2367344, gi:2367346, gi:2367349, gi:2367351, gi:2367352, gi:1790563, gi:1790574, gi:1790582, gi:2367354, gi:1790607, gi:2367356, gi:2367357, gi:1790649, gi:2367360, gi:1790670, gi:2367361, gi:2367366, gi:1790711, gi:2367368, gi:1790732, gi:2367369, gi:2367372, gi:2367374, gi:1790777, gi:1790789, gi:2367375, gi:2367377, gi:2367380, gi:2367382, gi:2367383, gi:1790858, gi:6626251.
Current U00096 annotation updates are derived from EcoGene http://ecogene.org. Suggestions for updates can be sent to Dr. Kenneth Rudd (krudd@miami.edu). These updates are being generated from a collaboration that also includes ASAP/ERIC, the Coli Genetic Stock Center, EcoliHub, EcoCyc, RegulonDB and UniProtKB/Swiss-Prot.
FEATURES Location/Qualifiers
source 1..1347
/organism="Escherichia coli str. K-12 substr. MG1655"
/mol_type="genomic DNA"
/strain="K-12"
/sub_strain="MG1655"

```
                     /db_xref="taxon:511145"
     gene            7..1347
                     /gene="fadL"
                     /locus_tag="b2344"
                     /gene_synonym="ECK2338"
                     /gene_synonym="JW2341"
                     /gene_synonym="ttr"
                     /db_xref="EcoGene:EG10280"
     CDS             7..1347
                     /gene="fadL"
                     /locus_tag="b2344"
                     /gene_synonym="ECK2338"
                     /gene_synonym="JW2341"
                     /gene_synonym="ttr"
                     /function="enzyme; Transport of small molecules;
                     Carbohydrates, organic acids, alcohols"
                     /note="long-chain fatty acid transport protein (outer
                     membrane flp protein);
                     GO_component: GO:0009274 - peptidoglycan-based cell wall;
                     GO_component: GO:0009279 - cell outer membrane;
                     GO_process: GO:0019395 - fatty acid oxidation"
                     /codon_start=1
                     /transl_table=11
                     /product="long-chain fatty acid outer membrane
                     transporter"
                     /protein_id="AAC75404.2"
                     /db_xref="GI:145693163"
                     /db_xref="ASAP:ABE-0007740"
                     /db_xref="UniProtKB/Swiss-Prot:P10384"
                     /db_xref="EcoGene:EG10280"
                     /translation="MSQKTLPTKSALAVAVALISTQAWSAGFQLNEFSSSGLGRAYSG
                     EGAIADDAGNVSRNPALITMPDRPTFSAGAVYIDPDVNISGTSPSGRSLKADNIAPTA
                     WVPNMHFVAPINDQFGWGASITSNYGLATEFNDTYAGGSVGGTTDLETMNLNLSGAYR
                     LNNAWSFGLGFNAVYARAKIERFAGDLGQLVAGQIMQSPAGQTQQGQALAATANGIDS
                     NTKIAHLNGNQWGFGWNAGILYELDKNNRYALTYRSEVKIDFKGNYSSDLNRAFNNYG
                     LPIPTATGGATQSGYLTLNLPEMWEVSGYNRVDEQWAIHYSLAYTSWSQFQQLKATST
                     SGDTLFQKHEGFKDAYRIALGTTYYYDDNWTFRTGIAFDDSPVPAQNRSISIPDQDRF
                     WLSAGTTYAFNKDASVDVGVSYMHGQSVKINEGPYQFESEGKAWLPGTNFNYAF"
     mat_peptide     82..1344
                     /gene="fadL"
                     /locus_tag="b2344"
                     /gene_synonym="ECK2338"
                     /gene_synonym="JW2341"
                     /gene_synonym="ttr"
                     /product="long-chain fatty acid outer membrane
                     transporter"
                     /experiment="N-terminus verified by Edman degradation;
                     PMID 1987139,9119048"
ORIGIN
        1 atggtcatga gccagaaaac ccctgtttaca aagtctgctc tcgcagtcgc agtggcactt
       61 atctccaccc aggcctggtc ggcaggcttt cagttaaacg aatttrcrtc ctctggcctg
      121 ggccgggcct attcagggga aggcgcaatt gccgatgatg caggtaacgt cagccgtaac
      181 cccgcattga ttactatgtt tgaccgcccg acatttttctg cgggtgcggt ttatattgac
      241 ccggatgtaa atatcagcgg aacgtctcca tctggtcgta gcctgaaagc cgataacatc
      301 gcgcctacgg catgggttcc gaacatgcac tttgttgcac cgattaacga ccaatttggt
      361 tggggcgctt ctattacctc taacnatggt ctggctacag agtttaacga tacttatgca
      421 ggcggctctg tcgggggtac aaccgacctt gaaaccatga acctgaactt aagcggtgcg
      481 tatcgcttaa ataatgcatg gagcttttggt cttggtttca acgccgtcta cgctcgcgcg
      541 aaaattgaac gtttcgcagg cgatcrgggg cagttggttg ctggccaaat tatgcaatct
      601 cctgctggcc aaactcagca agggcaagca ttggcagcta ccgccaacgg tattgacagt
      661 aataccaaaa tcgctcatct gaacggtaac cagtgggget ttggctggaa cgccggaatc
      721 ctgtatgaac tggataaaaa taaccgctat gcactgacct accgttctga agtgaaaatt
      781 gacttcaaag gtaactacag cagcgatctt aatcgtgcgt ttaataacta cggtttgcca
      841 attcctaccg cgacaggtgg cgcaacgcaa tcgggttatc tgacgctgaa cctgcctgaa
      901 atgtgggaag tgtcaggtta taaccgtgtt gatccacagt gggcgattca ctatagccrg
      961 gcttacacca gctggagtca gttccagcag ctgaaagcga cctcaaccag tggcgacacg
     1021 ctgttccaga aacatgaagg ctttaaagat gcttaccgca tcgcgttggg taccacttat
     1081 tactacgatg ataactggac cttccgtacc ggtatcgcct ttgatgacag cccagttcct
     1141 gcacagaatc gttctatctc cattccggac caggaccgtt tctggctgag tgcaggtacg
     1201 acttacgcat ttaataaaga tgcttcagtc gacgttggtg tttcttatat gcacggtcag
     1261 agcgtgaaaa ttaacgaagg cccataccag ttcgagtctg aaggtaaagc ctggctgttc
     1321 ggtactaact ttaactacgc gttctga
//
```

EXHIBIT B

Archives of Biochemistry and Biophysics
Vol. 377, No. 2, May 15, pp. 324–333, 2000
doi:10.1006/abbi.2000.1794, available online at http://www.idealibrary.com on IDEAL®

The Amino-Terminal Region of the Long-Chain Fatty Acid Transport Protein FadL Contains an Externally Exposed Domain Required for Bacteriophage T2 Binding

Gaetano Cristalli, Concetta C. DiRusso, and Paul N. Black[1]
Center for Cardiovascular Sciences, The Albany Medical College, Albany, New York 12208

Received December 6, 1999, and in revised form February 19, 2000

The fatty acid transport protein FadL from *Escherichia coli* is predicted to be rich in β-structure and span the outer membrane multiple times to form a long-chain fatty acid specific channel. Proteolysis of FadL within whole cells, total membranes, and isolated outer membranes identified two trypsin-sensitive sites, both predicted to be in externally exposed loops of FadL. Amino acid sequence analysis of the proteolytic fragments determined that the first followed R^{93} and yielded a peptide beginning with ^{94}S-L-K-A-D-N-I-A-P-T-A^{104} while the second followed R^{384} and yielded a peptide beginning with ^{385}S-I-S-I-P-D-Q-D-R-F-W^{395}. Proteolysis using trypsin eliminated the bacteriophage T2 binding activity associated with FadL, suggesting the T2 binding domain within FadL requires elements within one of these extracellular loops. A peptide corresponding to the amino-terminal region of FadL ($FadL^{28-160}$) was purified and shown to inactivate bacteriophage T2 in a concentration-dependent manner, supporting the hypothesis that the amino-proximal extracellular loop of the protein confers T2 binding activity. Using an artificial neural network (NN) topology prediction method in combination with Gibbs motif sampling, a predicted topology of FadL within the outer membrane was developed. According to this model, FadL spans the outer membrane 20 times as antiparallel β-strands. The 20 antiparallel β-strands are presumed to form a β-barrel specific for long-chain fatty acids. On the basis of our previous studies evaluating the function of FadL using site-specific mutagenesis of the *fadL* gene, proteolysis of FadL within outer membranes, and studies using the $FadL^{28-160}$ peptide, the predicted extracellular regions between β-strands 1 and 2 and β-strands 3 and 4 are expected to contribute to a domain of the protein required for long-chain fatty acid and bacteriophage T2 binding. The first trypsin-sensitive site (R^{93}) lies between predicted β-strands 3 and 4 while the second (R^{384}) is between β-strands 17 and 18. The trypsin-resistant region of FadL is predicted to contain 13 antiparallel β-strands and contribute to the long-chain fatty acid specific channel. © 2000 Academic Press

Key Words: membrane; protein; long-chain fatty acid; transport.

Imported fatty acids and fatty acid derivatives influence a wide variety of cellular processes, including fatty acid and phospholipid synthesis, organelle inheritance, vesicle fusion, protein export, protein modification, enzyme activation or deactivation, cell signaling, membrane permeability, bacterial pathogenesis, and transcriptional control (1–14). Thus it stands to reason that specific systems exist to regulate the import and/or export of these compounds. The cell is presented with a formidable challenge to transport exogenous long-chain fatty acids in part due to the low concentration of free fatty acids found within the environment and extracellular milieu and in part due to the diversity and selective permeability of biological membranes. Information gleaned over the past 15 years supports the hypothesis that the transport of exogenous long-chain fatty acid into cells occurs by a protein-mediated process. This hypothesis is supported by the identification of specific membrane-bound proteins that appear to be required for long-chain fatty acid transport.

Four distinct proteins believed to be involved in long-chain fatty acid transport have been described. The first is the outer membrane-bound fatty acid binding and transport protein FadL found in *Escherichia coli* and presumed to be present in most gram-negative

[1] To whom correspondence should be addressed. Fax: (518) 262-8101. E-mail: blackp@mail.amc.edu.

0003-9861/00 $35.00

bacteria (15). FadL functions with an inner membrane associated fatty acyl-CoA synthetase (FACS)[2] to facilitate the vectorial transport of long-chain fatty acids (15). It is generally held on the basis of genetic and functional data that transport and activation of long-chain fatty acids in this system are tightly coupled processes (15 and references therein). The second membrane-bound protein identified is fatty acid translocase (FAT, CD36) (16). FAT can be specifically modified with sulfo-*N*-succinimidyl oleate, which in turn blocks long-chain fatty acid transport. This protein has been described in a number of different eukaryotic cell types and is a member of a large family of scavenger proteins (16). The third protein, designated FABPpm (fatty acid binding protein–plasma membrane bound), appears to be peripherally associated with the membrane and is identical to mitochondrial aspartate aminotransferase, suggesting it may have a dual function (17, 18). The last fatty acid transport protein (FATP) was identified on the basis of functional and genetic studies in adipocytes and yeast. FATP is a member of the adenylate-forming superfamily of enzymes that include the fatty acyl-CoA synthetases. Evidence to date suggests that FATP and FACS act in concert to facilitate long-chain fatty acid transport (19–21). Despite the identification of the different proteins involved in fatty acid transport, little is known about their specific roles in this process, mechanisms of action, or structure.

Our laboratory has been instrumental in defining the components of, and evaluating the mechanism of, fatty acid transport in *E. coli* (15). In this system, the outer membrane long-chain fatty acid transport protein FadL (encoded by the *fadL* gene) functions in concert with the inner membrane associated fatty acyl-CoA synthetase (encoded by the *fadD* gene) to promote the vectorial transport of long-chain fatty acids. The long-chain fatty acid binding and transport functions associated with FadL are experimentally distinguishable. Long-chain fatty acid transport is routinely measured in a whole-cell system containing both wild-type FadL and FACS. When the FACS structural gene is deleted, transport becomes inoperable and a long-chain fatty acid binding activity specific to FadL can be measured. In general, the long-chain fatty acid binding activity of FadL is specifically disrupted by mutations encoding the amino-terminal region of the protein while the transport activity is disrupted by mutations corresponding to the carboxyl-terminal region (22–24). Furthermore, evidence from these mutagenesis studies supports the proposal that there is a conformationally sensitive region linking these two regions of FadL (22). The amino-terminal region of FadL associated with long-chain fatty acid binding also appears to overlap the region required for binding bacteriophage T2 (22, 24). The characteristic heat-modifiable property of FadL is contained within the carboxyl region of the protein (22).

FadL binds exogenous long-chain fatty acids by a high-affinity process requiring both the acyl chain and the carboxylate. The binding of long- but not medium-chain fatty acids by FadL suggests the length of the hydrocarbon tail of the substrate defines binding specificity (25). Oleoyl alcohol and methyl oleate are unable to compete for FadL-specific binding of [^{3}H]oleate, arguing the carboxylate of the long-chain fatty acid also contributes to binding (24). The aim of the present work was to develop a topological map of FadL consistent with the data previously obtained by directed mutagenesis as summarized above. Studies using limited proteolysis and peptide analyses were used to investigate the membrane topology and further define the functional domains of the bacterial fatty acid transport protein FadL. These data support the hypothesis that FadL traverses the outer membrane a number of times and contains specific elements within the amino terminus of the protein that are involved in the binding of bacteriophage T2. In addition, these studies have identified a 289-amino-acid residue trypsin-resistant fragment of FadL, which is hypothesized to represent the majority of a membrane-bound long-chain fatty acid specific channel. The data accumulated here together with previous mutational analyses were compared to a topological map of FadL based largely on the 2D structural prediction methods employing a neural network developed by Diederichs *et al.* (27).

MATERIALS AND METHODS

Bacterial strains, bacteriophage T2, and growth conditions. The bacterial strains used in these studies were K12 (prototroph), E15 (*fadL ompF*), and BL21 (λDE3/pLysS). Bacteria were routinely grown to mid-log phase in Luria broth (LB) or minimal medium E supplemented with vitamin B_1 and the appropriate carbon source at 37°C with aeration. When required to maintain plasmids, antibiotics were added to final concentrations of 100 μg of ampicillin/ml or 40 μg of chloramphenicol/ml. Bacterial growth was routinely monitored using a Klett–Summerson colorimeter equipped with a blue filter. Bacteriophage T2 was propagated on strain K12 and used as detailed previously (26).

Induction of FadL and preparation of outer membranes. Strain BL21(λDE3)/pLysS transformed with pN132 was grown to mid-log phase in minimal medium E supplemented with dextrose (30). FadL expression was induced with isopropyl β-D-thiogalactopyranoside (IPTG, 1 mM final concentration) and when necessary cells were treated with rifampicin (0.2 mg/1 ml) prior to labeling with [^{14}C]L-amino acids. Cells were subsequently harvested by centrifugation, washed in 10 mM Hepes, pH 7.0, 50 mM NaCl, and resuspended into the same buffer at a concentration of 5×10^8 cells/ml. The resuspended samples were cooled on ice and cells lysed by sonication. The

[2] Abbreviations used: NN, neural network; FACS, fatty acyl-CoA synthetase; FAT, fatty acid translocase; FABPpm, fatty acid binding protein–plasma membrane bound; FATP, fatty acid transport protein; IPTG, isopropyl β-D-thiogalactopyranoside; pfu, plaque-forming units.

cell lysate was clarified and total membranes in the resulting supernatant collected following centrifugation (75,000*g*; 30 min; TLS rotor, Beckman TL-100 ultracentrifuge). The membrane samples were resuspended in the same buffer and outer membranes separated from inner membranes as previously described using sucrose density gradients (31). The protein composition of the final outer membrane samples was monitored using SDS–polyacrylamide gel electrophoresis (32). Labeled FadL was detected using autoradiography.

For experiments evaluating the inactivation of bacteriophage T2, total and outer membranes containing unlabeled FadL were prepared as noted above from strain E15 (*fadL ompF*) transformed with pN130 (*fadL*$^+$, under the control of its native promoter) or pACYC177 (vector control).

Limited proteolysis of membranes containing FadL. Total membranes or isolated outer membranes containing ^{14}C-labeled FadL or FadL expressed from pN130 were subjected to limited proteolysis using increasing concentrations of trypsin. The protein concentration within the membrane samples was held constant between 100 and 125 μg in a total volume of 50 μl. Trypsin was added (final enzyme concentrations ranged from 0 to 200 μg/ml) to the FadL-containing membranes followed by incubation at 37°C for 30 min. The resultant peptides were resolved on 15% SDS–polyacrylamide gels. Following electrophoresis, the gels were dried and subjected to autoradiography. To test protection of FadL from proteolysis by bacteriophage T2, bacteriophage T2 was added to membrane sample to give a final concentration of 2×10^6 pfu/ml and samples incubated 12 h at 4°C prior to the addition of trypsin.

Peptide sequence analysis. In order to define the protease-resistant peptide(s) within FadL, membranes (100–125 μg of total protein) containing ^{14}C-labeled FadL were treated with 20 μg of trypsin for 30 min (37°C), peptides were separated on 15% SDS–polyacrylamide gels, and samples were transferred to an immobilon membrane as previously described (30). To test the heat-modifiable property of FadL, samples (native and trypsin-treated) were either boiled or held at room temperature prior to electrophoresis. The protease-resistant peptides were identified by autoradiography, excised from the immobilon membrane, and sequenced using an automated gas-phase protein sequenator.

Construction of pCG102 and expression and purification of 6×-His-FadL$^{28-160}$. The coding sequence of the amino-terminal region of FadL (encoding residues 28–160) was PCR amplified with UltimaTaq (Perkin-Elmer) using the forward primer L95 (5′-AATAGGATCCCAGGCTTTCAGTTAAACGAATTTTCTTCC-3′), the reverse primer L98 (5′-TAATAAGCTTGCTCCATGCATTATTTAAGCGATACG-3′), and the template pN155 (*fadL*$^+$) (23). The amplicon was digested with *Bam*H1 and *Hin*dIII (sites underlined), purified, and ligated into the T7 RNA polymerase responsive expression plasmid pRSET-C (Invitrogen). The final plasmid construction was designated pGC102 and encodes residues 28–160 of FadL fused in frame downstream to a hexameric histidine tag (6×-His-FadL$^{28-160}$).

For expression of 6×-His-FadL$^{28-160}$, strain BL21(λDE3)/pLysS was transformed with pGC102. The transformants were grown to mid-log phase in minimal medium E supplemented with dextrose. 6×-His-FadL$^{28-160}$ expression was induced as detailed above except the samples were not treated with rifampicin or labeled with [^{14}C]L-amino acids. Following induction and growth, cells were harvested by centrifugation, resuspended, and lysed as detailed above. The lysates were clarified by centrifugation and the 6×-His-FadL$^{27-160}$ peptide purified using Ni^{2+} chelation chromatography as previously defined (33). Expression and purification of 6×-His-FadL$^{28-160}$ were monitored using SDS–polyacrylamide gel electrophoresis.

Bacteriophage T2 inactivation. Bacteriophage T2 viability was monitored using the wild-type strain K12 as previously described (26). Isolated outer membranes prepared from a *fadL* strain, from a *fadL*$^+$ strain, and from a *fadL*$^+$ strain treated with trypsin as detailed above and the membrane containing 6×-His-FadL$^{28-160}$ were each incubated with 100 μl of bacteriophage T2 (1×10^6 plaque-forming units (pfu)/ml) at 4°C for 12 h with continuous rotation. The protein concentrations within the isolated outer membranes with no FadL, containing FadL with or without trypsin treatment, 6×-His-FadL$^{28-160}$, or ovalbumin (protein control) ranged between 0.1 and 100 μg/100 μl. The samples were subjected to centrifugation and supernatants assayed for bacteriophage T2 activity. To assay bacteriophage viability, the serial dilutions of the supernatants (100 μl) were added to 100 μl of strain K12 (grown to mid-log phase), the samples were incubated at 37°C for 30 min, soft agar was added, and the samples were plated on LB. Plaques were counted after 12 h of incubation at 37°C. The number of plaques with no FadL added was defined as 100% and all subsequent data adjusted accordingly. Data are presented as % pfu remaining following bacteriophage T2 inactivation, where 100% is equivalent to 1×10^6 pfu/ml. The data presented are from four independent experiments.

Computer modeling of FadL to predict membrane topology. The topology of FadL within the outer membrane was predicted using the artificial neural network (NN) algorithm of Diederichs *et al.* (27; http://loop8.biologie.uni-konstanz.de/~kay/om_topo_predict.html). Secondary structural predictions of FadL were also generated using the PHD algorithm of Rost and Sander (28; http://www.embl-heidelberg.de/predictprotein/predictprotein.html). Data identifying regions of FadL that are likely to form β-strands using Gibbs motif sampling have been previously published by Neuwald *et al.* (29).

General methods. Methods for DNA sequencing, restriction, ligation, and transformation followed established protocols (34). PCR amplification was performed using a Thermolyne Amplitron II with the indicated primers. Protein concentrations were estimated with the Bradford protein assay (Pierce), using bovine serum albumin as a standard.

RESULTS

In previous work we hypothesized the amino terminus of FadL specifically contributes to the binding of exogenous long-chain fatty acids while the carboxyl-terminal region specifically contributes to transport (22–24). Of particular note was the characterization of several linker mutations within *fadL* corresponding to carboxyl-terminal regions of the protein that resulted in defective transport and those corresponding to amino-terminal regions of the protein that resulted in defective binding and transport (22). In addition, several insertions and substitutions corresponding to the amino terminus of the protein were defective in binding bacteriophage T2 while none corresponding to the carboxyl end of the protein were defective for this activity (22–24). From these data, we presumed the amino-terminal region of FadL was involved in fatty acid and bacteriophage T2 binding and that this region contributed to a surface-exposed domain. In contrast, the region involved in fatty acid transport was suggested to be membrane-bound. In order to further test this hypothesis, we employed proteolysis of FadL within the outer membrane coupled with functional analyses, studies using an amino-terminal FadL peptide, and topological predictions of FadL using artificial neural networks and Gibbs motif sampling.

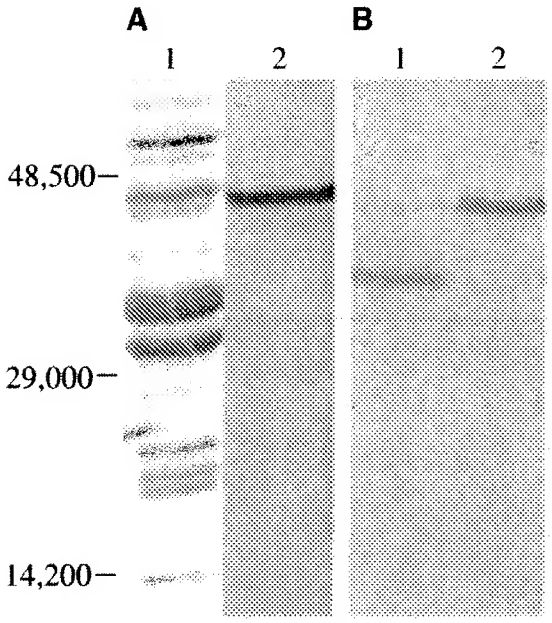

FIG. 1. T7 RNA polymerase-responsive expression of FadL and targeting to the outer membrane. (A) Lane 1, isolated outer membranes containing FadL; lane 2, autoradiograph of lane 1 showing that FadL can be specifically labeled with [^{14}C]L-amino acids. (B) Autoradiograph showing that FadL, expressed and targeted to the outer membrane, retains its characteristic heat-modifiable property Lane 1, outer membrane samples prepared at room temperature; lane 2, outer membrane samples prepared at 100°C prior to SDS–PAGE. Molecular weight standards are shown on the left.

Induction, specific labeling with ^{14}C, and targeting of FadL to the outer membrane. In order to investigate the topology of FadL within the outer membrane, it was first necessary to develop a system where the protein was enriched in the outer membrane and specifically labeled to aid identification. The FadL expression plasmid, pN132, contains the entire *fadL* gene under the control of a T7 RNA polymerase responsive promoter. Using the bacterial strain BL21(λDE3)/pLysS transformed with pN132, FadL was expressed at a high level and correctly targeted to the outer membrane. When *E. coli* RNA polymerase was inhibited with rifampicin, the only protein made was FadL, which was under the control of the rifampicin-resistant T7 RNA polymerase responsive promoter. Addition of [^{14}C]L-amino acids as the only source of amino acids in the growth media resulted in specific labeling of the target protein, FadL (Fig. 1A). One parameter, which we routinely use to assess whether FadL is appropriately folded within the outer membrane, is its characteristic heat-modifiable property (35). FadL expressed from pN132 is specifically labeled, is correctly targeted to the outer membrane, and maintains its characteristic heat-modifiable property (Fig. 1B).

Proteolysis of FadL within isolated outer membranes defines a protease-resistant fragment. Isolated outer membranes containing ^{14}C-labeled FadL were treated with increasing concentrations of trypsin for 30 min at 37°C (Fig. 2). Mature FadL (residues 28–448) contains 27 potential trypsin cleavage sites. As the concentration of trypsin increased, the intensity of the 43,000 M_r FadL band decreased. This was accompanied by the appearance of a 35,000 M_r FadL peptide followed by the appearance of a 29,500 M_r peptide. These results suggested that the trypsinolysis of FadL occurred in a stepwise fashion, initially yielding a peptide with an M_r of 35,000 followed by a peptide with an M_r of 29,500. As no peptides smaller than 29,500 M_r were detected, these results are consistent with the conclusion that the 29,500 M_r peptide of FadL is resistant to proteolysis. The 29,500 M_r peptide was not further degraded when incubated with trypsin for up to 18 h (data not shown). The trypsin-resistant property of this FadL peptide may be the result of both protection by the outer membrane and the tertiary structure arising from the predicted multiple transmembrane β-strands. The 29,500 M_r FadL peptide could also be generated in whole cells following specific labeling and treatment with trypsin, supporting the notion that the trypsin-sensitive sites in FadL reside at the outer membrane surface (data not shown). The 29,500 M_r FadL peptide is speculated to represent the majority of membrane-bound region of the protein comprising the long-chain fatty acid specific channel.

The data demonstrated FadL was cleaved in a stepwise fashion, first yielding a 35,000 M_r peptide followed by a 29,500 M_r peptide. As noted above, the mature form of FadL (residues 28–448) contains 27 potential trypsin cleavage sites. Using these as a guide, we predicted that the sites following R^{93} and R^{162} would give rise to the 29,500 M_r peptide in a sequential fashion.

In order to define the trypsin cleavage site giving rise to the 29,500 M_r peptide, outer membranes containing

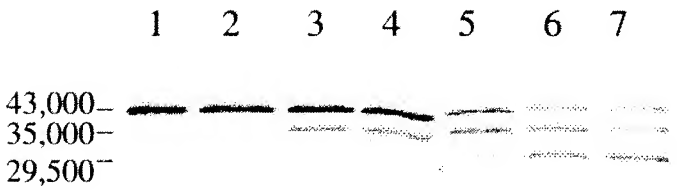

FIG. 2. ^{14}C-Labeled FadL peptides within the outer membrane following proteolysis with trypsin separated on 15% SDS–polyacrylamide gels and identified by autoradiography. Lane 1, no trypsin; lanes 2–7, trypsin at 1, 2, 4, 6, 8, and 10 μg, respectively. The M_r of FadL and FadL peptides is noted on the left.

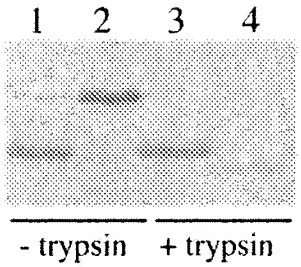

FIG. 3. Trypsin treatment of FadL does not generate a heat-modifiable peptide. Following expression and specific labeling with [^{14}C]L-amino acids, FadL was treated with trypsin under conditions that yielded the 29,500 M_r peptide (20 μg of trypsin for 30 min) and the samples prepared for SDS–PAGE and either held at room temperature (lanes 1 and 3) or boiled (lanes 2 and 4). Samples 3 and 4 were treated with trypsin as described under Materials and Methods. The band shown in lane 3 was transferred to an immobilon membrane and subjected to sequence analysis.

FadL were proteolyzed and resolved by SDS–polyacrylamide gel electrophoresis, and the 29,500 M_r peptide was transferred to an immobilon membrane. Automated Edman degradation defined the N-terminal sequence of this peptide as ^{94}S-L-K-A-D-N-I-A-P-T-A^{104}, corresponding to the first predicted trypsin cleavage site following R^{93}. There was no evidence that cleavage was taking place at the second predicted site (following R^{162}), supporting the notion that this region of the protein is not accessible to the protease. Since cleavage following R^{93} would result in a peptide with an M_r of 35,000–36,000, we reasoned that there must be a second, carboxyl-terminal trypsin-accessible site, which upon cleavage would yield the 29,500 M_r peptide. By comparing the potential trypsin cleavage sites predicted by computer analysis of the primary amino acid sequence of FadL as a guide, we hypothesized the second cleavage site must occur after R^{384} or R^{393} to give the 29,500 M_r peptide.

We initially tested whether the protein, following proteolysis with trypsin, resulted in a heat-modifiable peptide (35). To our surprise, we found the proteolyzed protein, when treated with SDS at room temperature, had an M_r of 33,000, equivalent to the nonproteolyzed FadL, while the boiled sample resulted in the 29,500 M_r peptide (Fig. 3). These results suggested that despite proteolysis and treatment with SDS at room temperature, FadL retained sufficient tertiary structure to run as a 33,000 M_r protein. With this in mind, we transferred the 33,000 M_r protein to immobilon following proteolysis and electrophoresis for sequence analysis using automated Edman degradation. This analysis identified three major peptides. The first, ^{28}A-G-F-Q-L-N-E-F-S-S-S^{38}, represents the N-terminal peptide of the mature protein; the second was the same as previously defined (^{94}S-L-K-A-D-N-I-A-P-T-A^{104}); and the final followed R^{384} (^{385}S-I-S-I-P-D-Q-D-R-F-W^{395}). On the basis of this information, we propose the 29,500 M_r protease-resistant peptide of FadL lies between residues 94 and 384 of FadL. It seems likely that this region of the protein contributes to an integral membrane component that forms the long-chain fatty acid specific channel.

Proteolysis of membrane-bound FadL in the presence of bacteriophage T2. FadL serves as an outer membrane receptor for bacteriophage T2. Previous work has identified mutations within *fadL* within the amino-terminal region (insertions between residues 40 and 41 and between residues 80 and 81, respectively) of the protein that are defective in bacteriophage T2 binding (22). On the basis of these data, we hypothesized the T2 binding site resides within this region of the protein and is externally exposed. Binding of T2 to FadL is therefore expected to protect this portion of the protein involved in receptor activity from digestion with trypsin. The proteolysis of FadL with isolated outer membranes was carried out in the presence of bacteriophage T2 (Fig. 4). These experiments showed the 35,000 M_r FadL peptide, and not the 29,500 M_r peptide, was produced, suggesting the bacteriophage particles partially protected FadL from proteolysis with trypsin. As our earlier studies showed that specific mutations within the amino terminus of the protein depressed bacteriophage T2 plating efficiency, we suspected the 35,000 M_r peptide resulted from trypsin cleavage at R^{384}, supporting the hypothesis that the T2 binding domain is found within the amino-terminal region of FadL (22). Thus on the basis of these data, we propose bacteriophage T2 bound to FadL specifically blocks trypsin accessibility to the amino-terminal region of the protein at position R^{93}.

Inactivation of bacteriophage T2 by FadL. In order to test the hypothesis that the bacteriophage T2 binding domain of FadL resides within the amino terminus of the protein, outer membranes were prepared from strain E15 (*ompF fadL*) transformed with pAYCY177 (control) or pN130 (*fadL*$^+$). The plasmid pN130 fully

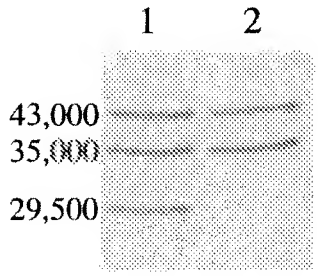

FIG. 4. Bacteriophage T2 partially protects FadL from trypsinolysis. Outer membranes containing ^{14}C-labeled FadL were prepared and incubated with buffer (A) or with 1×10^6 pfu/ml of bacteriophage T2 (B) prior to incubation with trypsin. Samples were separated on 15% SDS–polyacrylamide gels and subjected to autoradiography.

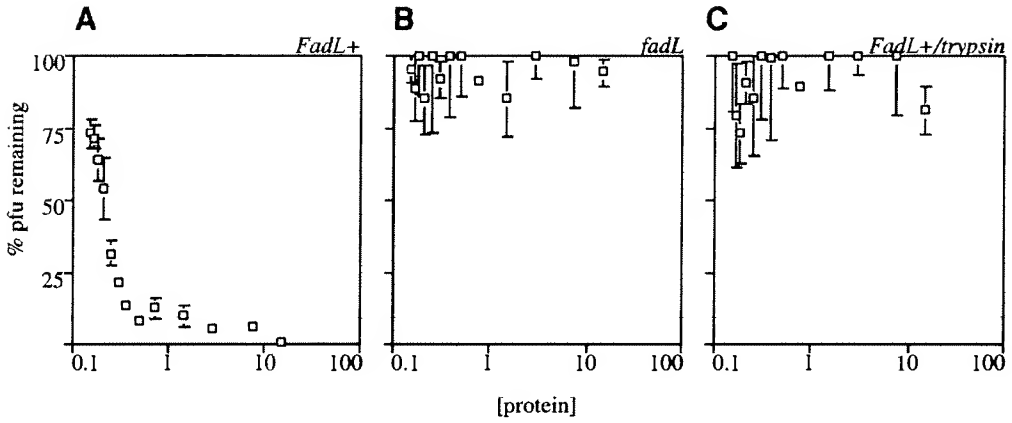

FIG. 5. Bacteriophage T2 binding to FadL is eliminated following trypsinolysis of outer membranes containing FadL. (A) Percentage of plaque-forming units (pfu) remaining following incubation with increasing concentrations of outer membranes containing FadL. (B) Percentage of pfu remaining following incubation with increasing concentrations of outer membranes prepared from a *fadL* strain. (C) Percentage of pfu remaining following incubation with increasing concentration of outer membranes containing FadL and incubated with trypsin. Protein concentrations are given in μg of total protein/ml and bacteriophage T2 was held constant at 1×10^6 pfu/ml (100% pfu corresponds to 1×10^6 bacteriophage T2 particles).

restores growth of strain E15 in oleate minimal media and the ability to transport long-chain fatty acids at wild-type levels. Outer membranes lacking or containing FadL were incubated with bacteriophage T2 (1×10^6 pfu/ml) for 12 h at 4°C. The membrane-bound T2 particles in both samples were removed by centrifugation and the supernatants assayed for bacteriophage T2 by monitoring the efficiency of plating on the wild-type strain K12. As illustrated in Fig. 5A, membranes containing FadL could efficiently remove bacteriophage T2 in a protein concentration dependent manner. When outer membranes were prepared from the *fadL* strain E15 transformed with only the plasmid vector, no such inactivation of bacteriophage T2 was observed (Fig. 5B).

Using this experimental approach, we tested the effects of proteolysis of FadL on bacteriophage T2 binding. Purified outer membranes containing FadL were treated with trypsin as detailed above, extensively washed, and mixed with bacteriophage T2 (1×10^6 pfu/ml), and the supernatants were assayed for bacteriophage T2 activity. As illustrated in Fig. 7C, these membranes were unable to bind T2. In fact, these membranes appeared nearly identical to those lacking FadL (Fig. 5B). These observations were fully in support of the bacteriophage T2 proteolysis protection data.

The bacteriophage T2 binding domain of FadL resides within the FadL peptide 28–160. The data detailed above coupled with our previous mutagenesis studies on *fadL* supported the notion that the amino terminus of FadL contains sequence elements responsible for binding bacteriophage T2. In order to test this possibility, an expression plasmid encoding an amino-terminal proximal peptide of FadL was constructed. The expression plasmid, pGC102, encodes the FadL peptide corresponding to residues 28–160 of the protein preceded by a hexameric histidine tag (6×-His-FadL$^{28-160}$). 6×-His-FadL$^{28-160}$ was expressed at high levels following induction with IPTG (Fig. 6A) and could be purified using Ni^{2+} chelation chromatography (Fig. 6B).

6×-His-FadL$^{28-160}$ was tested for ability to inactivate bacteriophage T2 as described under Materials and Methods. As illustrated in Fig. 7, efficiency of plating on strain K12 decreases sharply with increasing concentrations of 6×-His-FadL$^{28-160}$. These data are consistent with this peptide specifically inactivating bacteriophage T2. As a control, commercially available ovalbumin was used at the same concentrations. Increasing the concentration of ovalbumin had no effect on the efficiency of plating bacteriophage T2 (Fig. 7).

FIG. 6. Expression and purification of 6×-His-FadL$^{28-160}$. Lane 1, SDS–polyacrylamide gel of whole-cell extract following induction of 6×-His-FadL$^{28-160}$; lanes 2 and 3; aliquots of fractions eluting between 300 and 400 mM imidazole containing the purified protein.

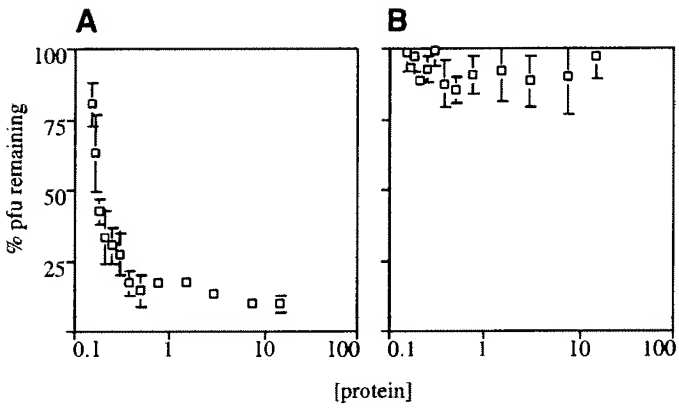

FIG. 7. Inactivation of bacteriophage T2 with 6×-His-FadL$^{28-160}$ (A); ovalbumin at the same protein concentrations was used as a control (B). Experimental details are the same as described in the legend to Fig. 6.

Development of a topological map of FadL within the outer membrane. On the basis of the studies described above and in conjunction with the results of site-specific mutagenesis of *fadL*, the amino terminus of the protein binds both bacteriophage T2 and long-chain fatty acids while the carboxyl terminus contributes to protein stability and fatty acid transport. We employed the 2D prediction methods using an artificial neural network developed by Diederichs *et al.* (27) to predict the topology of FadL within the outer membrane. This method is consistent with experimental topological data of a number of outer membrane proteins containing β-strands (27) and predicts FadL spans the outer membrane at least 20 times (Fig. 8). A second approach to evaluate outer membrane protein topology is Gibbs motif sampling (29). This method, using different indices of discrimination, identified six regions of FadL predicted to span the outer membrane as β-strands (29). These six regions correspond to membrane-spanning segments 3, 7, 16, 17, 19, and 20 noted in Fig. 8 expected based upon the 2D prediction methods. The two trypsin cleavage sites identified in this work (R^{93} and R^{384}) are predicted to be in externally exposed loops (II and IX, respectively).

There are a number of features of this predicted outer membrane topology which are supported by our previous data using site-specific mutagenesis of the *fadL* gene, our present data using proteolysis of FadL within the outer membrane, and our studies using the FadL$^{28-160}$ peptide. The extracellular domain between β-strands 3 and 4 is predicted to have α-helical character on the basis of the PHD algorithm of Rost and Sander (28). This putative external domain contains His^{110}, which we have shown is involved in long-chain fatty acid binding (24). The *fadLH1* (insertion of R-I between residues 40 and 41; in predicted β-strand 1) and *fadLH2* (insertion of D-F between residues 81 and 82; in predicted β-strand 3) alleles each result in altered FadL proteins that are defective in fatty acid binding (22). *fadLH1* results in a protein which is defective for bacteriophage T2 binding while *fadLH2* results in a protein which only slightly depresses bacteriophage T2 plating efficiency (22). As detailed above, a peptide including the region of FadL defective in these two alleles (FadL$^{28-160}$) specifically inactivates bacteriophage T2. Furthermore, disruption of this region of the protein upon proteolysis (Δ28–93) eliminates the bacteriophage T2 binding activity associated with the protein. The *fadLH3* allele (insertion of D-F between residues 238 and 239; in a periplasmic loop between β-strands 10 and 11) results in a protein with defective long-chain fatty acid binding but has moderate levels of transport. This differs from the three previous alleles that have very low levels of long-chain fatty acid binding and transport. The biochemical phenotype of *fadLH3* is consistent with the notion that the fatty acid specific channel is accessible, or "open." In this regard, the D-F insertion between residues 238 and 239 may have identified a region of FadL that is conformationally sensitive and upon fatty acid binding provides access to a fatty acid specific channel. The *fadL* alleles which result in defective fatty acid transport (while retaining either a wild-type or nearly wild-type long-chain fatty acid binding) are clustered toward the carboxyl terminus of the protein (includes *fadLS397N* and *fadLF448S*) (22, 23). The *fadLS1* allele encodes a protein (insertion of D-F between residues 410 and 411; in predicted β-strand 19) defective in long-chain fatty acid transport. This protein also lacks the characteristic heat-modifiable property of FadL, suggesting the membrane-spanning β-strand containing residues 410 and 411 is crucial for maintaining the tertiary structure of the mature protein (22). In addition, the *fadLD1* and *fadLD2* alleles (corresponding to 4 and 8 amino acid deletions in the carboxyl-terminal region of FadL, respectively) also result in proteins lacking the heat-modifiable property, suggesting that the carboxyl end of FadL is essential for maintaining the integrity of the protein within the outer membrane (23). Several *fadL* alleles corresponding to the carboxyl-terminal region of the protein (*fadLV410D* and *fadLP428A*) have lowered long-chain fatty acid binding and transport activities, suggesting this region also contributes to ligand binding (23).

DISCUSSION

The transport of long-chain fatty acids into *E. coli* occurs via a highly specific process that requires the outer membrane protein FadL. This protein is presumed to form a fatty acid specific channel and is hypothesized to contain amino-terminal proximal sequence elements involved in long-chain fatty acid and

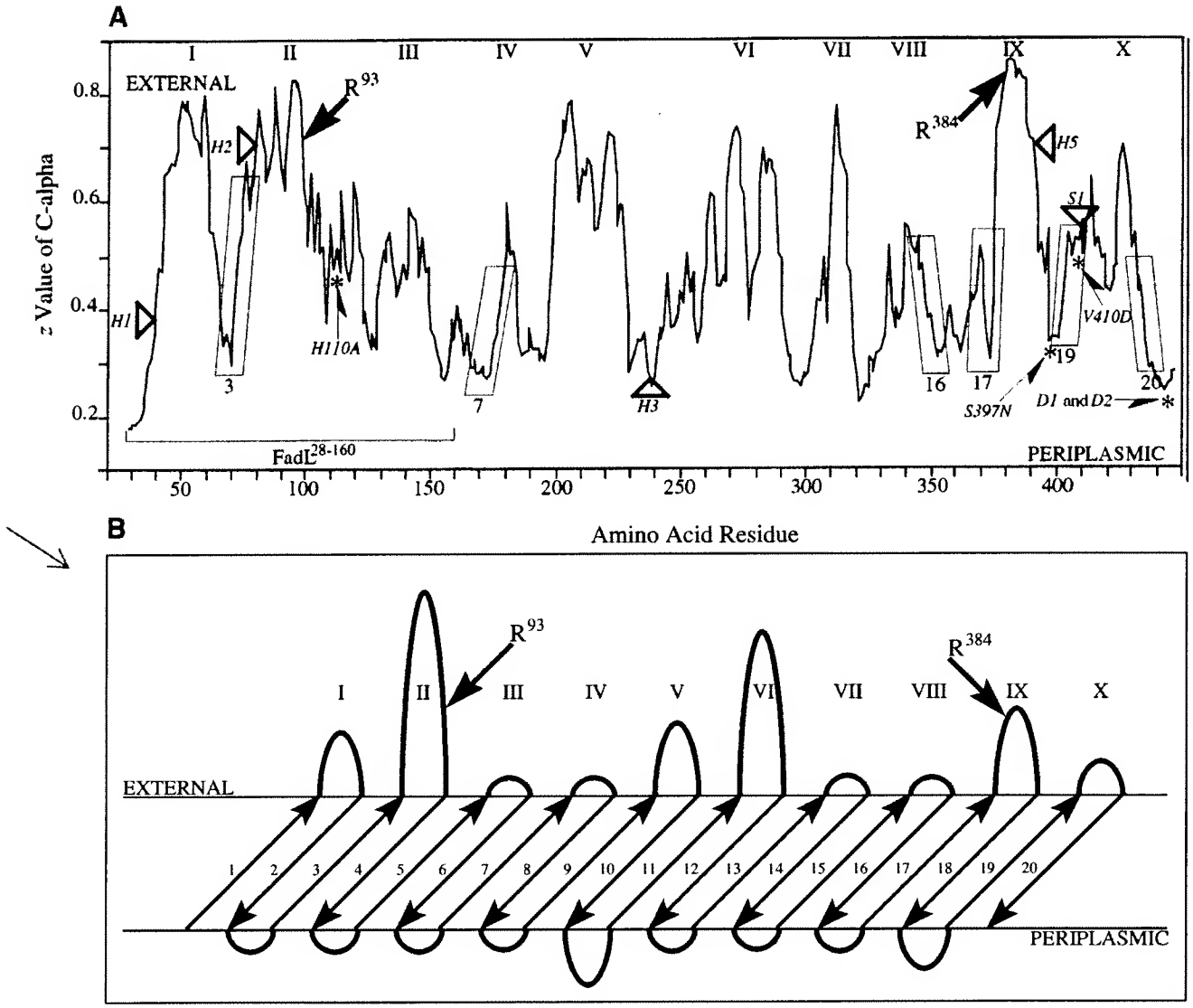

FIG. 8. (A) Topology plot for FadL from *E. coli* predicted using the artificial neural network developed by Diederichs *et al.* (27). Roman numerals (I–X) above the plot denote positions of NN-predicted extracellular loops with high z values of C-α. The boxes correspond to the regions of the protein predicted to have membrane-spanning β-strands based upon Gibbs motif sampling (28) and are numbered to correspond with predicted β-strains shown in B while the bold arrows denote the trypsin-sensitive sites. A number of mutations within *fadL* are also shown as reference and are discussed in the text (linker mutations *fadLH1* (*H1*), *fadLH2* (*H2*), *fadLH3* (*H3*), *fadLH5* (*H5*), and *fadLS1* (*S1*) are noted by the bold triangles and specific substitutions are noted by the asterisks and single-sided arrows. $FadL^{28-160}$ denotes the FadL peptide that specifically inactivates bacteriophage T2. (B).The predicted topology of FadL within the outer membrane. The predicted β-strands (shown as arrows) are numbered 1–20, the roman numerals (I–X) correspond to the same regions noted in A, and the bold arrows correspond to the trypsin-sensitive sites.

bacteriophage T2 binding. The proteolysis studies suggest at least three structural domains of FadL: (1) an amino-terminal protease sensitive domain required for bacteriophage T2 binding; (2) a carboxyl-terminal protease sensitive region proposed to be involved in facilitating long-chain fatty acid transport; and (3) a central, protease-resistant region predicted to be integral to the outer membrane. The predicted topology of FadL as illustrated in Fig. 8 using the 2D prediction methods developed by Diederichs *et al.* (27) coupled with previous data generated using Gibbs motif sampling is supported by the proteolysis and peptide analyses presented in the present work.

This predicted topology of FadL highlights several interesting features of this protein. Like other outer membrane proteins involved in nutrient transport, this protein is predicted to contain an even number of membrane-spanning antiparallel β-strands. The approximate positions of the tyrosine and phenylalanine residues in the predicted membrane-spanning segments

are consistent with their postulated roles in forming an aromatic girdle (36). On the basis of the predicted topology of FadL, an α-helical region that includes a glutamine-rich region (^{196}QIMQSPAGQTQQGQ^{209}) resides on the extracellular face (loop V) of the outer membrane. While the function of this stretch of glutamine residues is unknown, it is interesting to note that it is linked by β-strand 10 to the periplasmic loop that is postulated to be conformationally sensitive (22). This proposed periplasmic loop in FadL is defective in the *fadLH3* allele (insertion of D-F between residues 238 and 239) and results in a mutant protein that has an open, or accessible, long-chain fatty acid channel (22). FadLH3 confers long-chain fatty acid transport levels that are 40% wild type but has long-chain fatty acid binding levels that are only slightly above background (>5% wild-type binding).

Like most outer membrane proteins that form a β-barrel, the carboxyl end of FadL contains a terminal phenylalanine residue. Deletion of the terminal four or eight residues of FadL (*fadLD1* and *fadLD2*), resulting in a truncated form of FadL with F^{444} or F^{440} as the terminal residues, respectively, results in proteins that are unstable and thus unable to function in both binding and transport of long-chain fatty acids (23). Like other outer membrane proteins, this region of FadL may well interact with elements in the amino-terminal portion of the protein to stabilize what we presume is a long-chain fatty acid specific channel.

The proposed topology of FadL also agrees with the protease data generated in the present study. We have identified a 29,500 M_r trypsin-resistant peptide of FadL corresponding to the region of the protein from S^{94} to R^{384}. The trypsin cleavage sites following R^{93} and R^{384} are both predicted to be exposed at the external face of the outer membrane. R^{93} is presumed to lie between β-strands 3 and 4 while R^{384} is between β-strands 17 and 18. The region of FadL that is protease-resistant is likely to include the major components of the channel specific for long-chain fatty acids. The present data have further demonstrated the region of FadL contributing to the binding of bacteriophage T2 is trypsin-sensitive. Through the use of a FadL-specific peptide that corresponds to the amino-terminal region of the mature protein, we have shown that the bacteriophage T2 binding domain is contained within this region. These data are in complete agreement with previous mutagenesis studies demonstrating that mutations within the amino-terminal domain of FadL affect the efficiency of plating bacteriophage T2.

The long-chain fatty acid transport protein FadL represents the gate linking the import and activation of long-chain fatty acids to transcriptional control mediated through the fatty acyl-CoA-responsive transcription factor FadR (15, 37). The trafficking of exogenous long-chain fatty acids represents a simple, yet elegant, signal transduction pathway that allows the cell to optimize the expression or repression of genes in response to exogenous long-chain fatty acids. In this regard, FadL acts as an environmental sensor, which through the activity of fatty acyl-CoA synthetase allows the cell to respond to environmental fatty acids.

On the basis of information presented in this work, we presume that FadL is embedded in the outer membrane and facilitates the binding and transport of exogenous long-chain fatty acids. If the topology predicted for FadL is correct, elements within the amino-terminal region of the protein contribute to long-chain fatty acid binding. The long-chain fatty acid binding region of the protein, therefore, overlaps the region that we have shown is involved in binding bacteriophage T2. This topology also predicts that FadL assumes a tertiary conformation like other outer membrane proteins, resulting in the juxtaposition of the amino and carboxyl ends to form a β-barrel specific for long-chain fatty acids. It appears that FadL, like FhuA, contains elements within the amino-terminal region that contribute to substrate binding and elements that are conformationally sensitive (38).

Given the role of FadL in the uptake of long-chain fatty acids, one may question why such a system has evolved in *E. coli* and other gram-negative bacteria (for comparisons, refer to http://www.tigr.org). The answer must lie in maximizing the response to the nutritional needs of the cell by specifically adjusting the metabolic circuitry required for fatty acid transport, activation, and degradation. As importantly, these adjustments may provide a protective mechanism required for the cell, for example under conditions of stasis and stress and for pathogenesis. It has recently been shown that the expression of the fatty acid degradative genes in *E. coli* (including *fadL*) are induced during stasis, which, we presume, reflects a protective mechanism (39). Likewise it has been shown that *fadF* and *fadB* in *Salmonella typhimurium* are induced during early stages of pathogenesis, implying that the other genes required for fatty acid import, activation, and degradation are likely to be induced as well (10, 11). As *S. typhimurium* has a FadL homologue, its structural gene (*fadL*) is likely to be regulated in concert with *fadF* and *fadB* and thus play a pivotal role in pathogenesis. Again, this must reflect the generation of a protective mechanism for the cell that proceeds through fatty acid transport and activation to fatty acyl-CoA-responsive transcriptional control.

ACKNOWLEDGMENTS

This work was supported by the National Science Foundation (MCB-9816414). The Amino Acid Analyses and Peptide Sequencing Core Facility of the Wadsworth Center of the New York State Department of Public Health directed by Frank Maley and Li-Ming Chanchein provided peptide sequencing. We thank members of the

FATTT laboratory, Carmen Mannella and Eckhard Hofmann, for useful discussions during the course of this work.

REFERENCES

1. Hillgartner, F. B., Salati, L. M., and Goodridge, A. G. (1995) *Physiol. Rev.* **75**, 47–76.
2. Carmen, G. M., and Zeimetz, G. M. (1996) *J. Biol. Chem.* **27**, 13293–13296.
3. Warren, G., and Wickner, W. (1996) *Cell* **84**, 395–400.
4. Pfanner, N., Orci, L., Glick, B. S., Amherdt, M., Ardern, S. R., Malhotra, V., and Rothman, J. E. (1989) *Cell* **59**, 95–102.
5. Gordon, J. I., Duronio, R. S., Rudnick, D. A., Adams, S. P., and Gokel, G. W. (1991) *J. Biol. Chem.* **266**, 8647–8650.
6. McLaughlin, S., and Aderem, A. (1995) *Trends Biochem. Sci.* **20**, 270–276.
7. Fujimoto, Y., Tsunomori, M., Sumiya, T., Nishida, H., Sakuma, S., and Fujita, T. (1995) *Prostaglandins Leukot. Essent. Fatty Acids* **52**, 255–258.
8. Aihaud, G. P., Abumrad, N. A., Amri, E.-Z., and Grimaldi, P. A. (1994) *in* Fatty Acids and Lipids: Biological Aspects (Simopoulos, G. C., and Tremoli, E., Eds.), Karger Press, Basel.
9. Rich, G. T., Comerford, J. G., Graham, S., and Dawson, A. P. (1995) *Biochem. J.* **306**, 703–708.
10. Spector, M. P., DiRusso, C. C., Pallen, M. J., Garcia del Portillo, F., Dougan, G., and Finlay, B. B. (1999) *Microbiology* **145**, 15–31.
11. Mahan, M. J., Tobias, J. W., Slauch, J. M., Hanna, P. C., Collier, J. R., and Mekalanos, J. J. (1995) *Proc. Natl. Acad. Sci. USA* **92**, 669–639.
12. DiRusso, C. C., Heimert, T. L., and Metzger, A. K. (1992) *J. Biol. Chem.* **267**, 8685–8691.
13. Raman, N., and DiRusso, C. C. (1998) *J. Biol. Chem.* **273**, 22652–22659.
14. Hertz, R., Magenheim, J., Berman, I., and Bar-Tana, J. (1998) *Nature* **392**, 512–516.
15. DiRusso, C. C., Black, P. N., and Weimar, J. D. (1999) *Prog. Lipid Res.* **38**, 129–197.
16. Abumrad, N., Harmon, C., and Ibrahimi, A. (1998) *J. Lipid Res.* **39**, 2309–2318.
17. Stump, D. D., Shou, S.-L., and Berk, P. D. (1993) *Am. J. Physiol.* **265**, G894–G902.
18. Isola, L. M., Zhou, S.-L., Kiang, C.-L., Stump, D. D., Bradbury, M. W., and Berk, P. D. (1995) *Proc. Natl. Acad. Sci. USA* **92**, 9866–9870.
19. Schaffer, J. E., and Lodish, H. F. (1994) *Cell* **79**, 427–436.
20. Færgeman, N. J., DiRusso, C. C., Elberger, A., Knudsen, J., and Black, P. N. (1997) *J. Biol. Chem.* **272**, 8531–8538.
21. DiRusso, C. C., and Black, P. N. (1999) *Mol. Cell. Biochem.* **192**, 41–52.
22. Kumar, G. B., and Black, P. N. (1991) *J. Biol. Chem.* **266**, 1348–1353.
23. Kumar, G. B., and Black, P. N. (1993) *J. Biol. Chem.* **268**, 15469–15476.
24. Black, P. N., and Zhang, Q. (1995) *Biochem. J.* **310**, 389–394.
25. Black, P. N. (1990) *Biochim. Biophys. Acta* **1046**, 97–105.
26. Black, P. N. (1988) *J. Bacteriol.* **170**, 2850–2854.
27. Diederichs, K., Freigang, J., Umhau, S., Zeth, K., and Breed, J. (1998) *Protein Sci.* **7**, 2413–2420.
28. Rost, B., and Sander, C. (1993) *J. Mol. Biol.* **232**. 584–599.
29. Neuwald, A. F., Liu, J. S., and Lawrence, C. E. (1995) *Protein Sci.* **4**, 1618–1632.
30. Black, P. N. (1991) *J. Bacteriol.* **173**, 435–442.
31. Osborn, M. J., Gander, J. E., Parisi, E., and Carson, J. (1972) *J. Biol. Chem.* **247**, 3962–3972.
32. Laemmli, U. K. (1970) *Nature* **22**, 680–685.
33. Black, P. N., Zhang, Q., Weimar, J. D., and DiRusso, C. C. (1997) *J. Biol. Chem.* **272**, 4896–4903.
34. Maniatis, T., Fritsch, E. F., and Sambrook, J. (1982) Molecular Cloning: A Laboratory Manual, Cold Spring Harbor Laboratory Press, Cold Spring Harbor, NY.
35. Black, P. N., Said, B., Ghosn, C., Beach, J. V., and Nunn, W. D. (1987) *J. Biol. Chem.* **262**, 1412–1419.
36. Schultz, G. (1994) *in* Bacterial Cell Wall (Ghuysen, J.-M., and Hakenbeck, R., Eds.), pp. 343–362, Elsevier, Amsterdam.
37. DiRusso, C. C., Heimert, T. L., and Metzger, A. K. (1993) *Mol. Microbiol.* **7**, 311–322.
38. Ferguson, A. D., Hofmann, E., Coulton, J. W., Dieterichs, K., and Welte, W. (1998) *Science* **282**, 2215–2220.
39. Farewell, A., Diez, A. A., DiRusso, C. C., and Nystrom, T. (1996) *J. Bacteriol.* **178**, 6443–6450.

EXHIBIT C

Display of Lipase on the Cell Surface of *Escherichia coli* Using OprF as an Anchor and Its Application to Enantioselective Resolution in Organic Solvent

Seung Hwan Lee,[1] Jong-il Choi,[1] Mee-Jung Han,[1,2] Jong Hyun Choi,[1,2] Sang Yup Lee[1,2]

[1]Metabolic and Biomolecular Engineering National Research Laboratory, Department of Chemical & Biomolecular Engineering, and BioProcess Engineering Research Center, Korea Advanced Institute of Science and Technology, 373-1 Guseong-dong, Yuseong-gu, Daejeon 305-701, Republic of Korea; telephone: +82-42-869-3930; fax: +82-42-869-8800; e-mail: leesy@kaist.ac.kr
[2]Department of BioSystems and Bioinformatics Research Center, Korea Advanced Institute of Science and Technology, 373-1 Guseong-dong, Yuseong-gu, Daejeon 305-701, Republic of Korea

Received 16 July 2004; accepted 5 November 2004

Published online 28 February 2005 in Wiley InterScience (www.interscience.wiley.com). DOI: 10.1002/bit.20399

Abstract: We have developed a new cell surface display system using a major outer membrane protein of *Pseudomonas aeruginosa* OprF as an anchoring motif. *Pseudomonas fluorescens* SIK W1 lipase gene was fused to the truncated *oprF* gene by C-terminal deletion fusion strategy. The truncated OprF-lipase fusion protein was successfully displayed on the surface of *Escherichia coli*. Localization of the truncated OprF-lipase fusion protein was confirmed by western blot analysis, immunofluorescence microscopy, and whole-cell lipase activity. To examine the enzymatic characteristics of the cell surface displayed lipase, the whole-cell enzyme activity and stability were determined under various conditions. Cell surface displayed lipase showed the highest activity at 37°C and pH 8.0. It retained over 80% of initial activity after incubation for a week in both aqueous solution and organic solvent. When the *E. coli* cells displaying lipases were used for enantioselective resolution of racemic 1-phenylethanol in hexane, (*R*)-phenyl ethyl acetate was successfully obtained with the enantiomeric excess of greater than 96% in 36 h of reaction. These results suggest that *E. coli* cells displaying lipases using OprF as an anchoring motif can be employed for various biotechnological applications both in aqueous and nonaqueous phases.

Keywords: enantioselective resolution; cell surface display; recombinant *E. coli*; OprF; lipase; whole-cell biocatalyst

INTRODUCTION

Recently, enzymatic transformation of chemicals for the production of enantiomerically pure compounds has been drawing much research attention (Burton et al., 2002; Koeller and Wong, 2001). Numerous enzymes including amidase, lipase, protease, epoxide hydrolase, cytochrome P_{450}, peroxidase, monooxygenase, aldolase, decarboxylase, and dehydrogenase have been applied in various enantioselective reactions (Drauz and Waldmann, 2002; Patel, 2000). Lipase (triacylglycerol acylhydrolase, EC 3.1.1.3) has been the most popular enzyme for this purpose, as it catalyzes enantioselective hydrolysis and transesterification reaction using a broad spectrum of substrates (Jaeger et al., 1999). Many enantiomerically pure compounds have been produced by regio- and enantioselective reactions catalyzed by lipase such as kinetic resolution of 1-phenylethanol (Schöfer et al., 2001) and α-methylene β-lactams (Adam et al., 2000), and dynamic kinetic resolution of hemiaminals (Sharfuddin et al., 2003) and esters (Pàmies and Bäckvall, 2002). However, the use of crude lipases often causes problems such as reduced enantioselectivity and product yield and the presence of impurities. The use of a highly purified enzyme or an immobilized enzyme can partially solve these problems. However, enzyme instability and the more expensive process become new problems (Lalonde et al., 1997). As an alternative, cell surface displayed lipase can be used as an enantioselective biocatalyst (Matsumoto et al., 2004).

Cell surface display allows display of peptides or proteins on the surface of microorganism by appropriately fusing them to surface anchoring motifs (Georgiou et al., 1997; Lee et al., 2003; Wittrup, 2001). The anchoring motifs that have been employed include various outer membrane proteins, lipoproteins, autotransporters, subunits of surface appendages, and S-layer proteins (Georgiou et al., 1997; Jung et al., 1998; Lee et al., 2003). Among these, outer

Correspondence to: Sang Yup Lee
Contract grant sponsors: Ministry of Commerce, Industry and Energy; Intelligence Bioinformatics and Application Center; LG; IBM; BK21; Center for Ultramicrochemical Process Systems
Contract grant number: TGW 10011093

membrane proteins have widely been used as anchoring motifs for the display of peptides and proteins because they have several merits such as efficient secretory signal, unique membrane-spanning structures providing fusion sites, and strong anchoring structures. Outer membrane proteins including OmpA, OprF, OmpS, FadL, LamB, PhoE, OmpC, and Lpp–OmpA have been successfully used as anchoring motifs for displaying various peptides and proteins (Benhar, 2001; Samuelson et al., 2002; Xu and Lee, 1999). However, only a few anchoring motifs have been able to display relatively large enzymes (Lee et al., 2003). Furthermore, each anchoring motif has been found to have different capacities in displaying proteins, which makes it necessary to develop a range of anchoring motifs for displaying proteins of various sizes and different characteristics (Lee et al., 2003).

The OprF is a major outer membrane protein of *Pseudomonas aeruginosa*. This protein functions as a nonspecific porin to allow the passage of small hydrophilic molecules, plays a structural role in maintaining cell shape and outer membrane integrity, and is required for growth under low osmolality (Nikaido et al., 1991; Rawling et al., 1995). The structure of OprF has been proposed to consist of three domains, the N-terminal forming β-barrel structure, a loop or hinge region, and the C-terminal associated with peptidoglycan (Rawling et al., 1998; Woodruff et al., 1986).

In this paper, we constructed a system for the display of *Pseudomonas fluorescens* SIK W1 lipase (49.9 kDa) using OprF as an anchoring motif, and examined the biocatalytic applications of recombinant *Escherichia coli* displaying lipase on the cell surface. As an important application, enantioselective transesterification of 1-phenylethanol in the nonaqueous phase was demonstrated (Fig. 1).

MATERIALS AND METHODS

Bacterial Strains and Growth Condition

E. coli XL10-Gold (Tet^r Δ(*mcrA*)*183* Δ (*mcrCB-hsdSMR-mrr*)*173 endA1 supE44 thi-1 recA1 gyrA96 relA1 lac* Hte [F′ *proAB lacI*^{q}*ZΔM15* Tn*10* (Tet^r) Amy Cam^r]; Stratagene Cloning System, La Jolla, CA) was used as a host strain for general cloning works and surface display studies. Recombinant cells were cultivated in Luria-Bertani (LB) medium (10 g/L bacto-tryptone, 5 g/L bacto-yeast extract, and 5 g/L NaCl) supplemented with 50 mg/L of ampicillin at 37°C and 250 rpm. For the production of recombinant proteins, cells were induced with 0.1 or 1 mM isopropyl-β-D-thiogalactopyranoside (IPTG) at the OD_{600} of 0.4 and further cultured for 4 h.

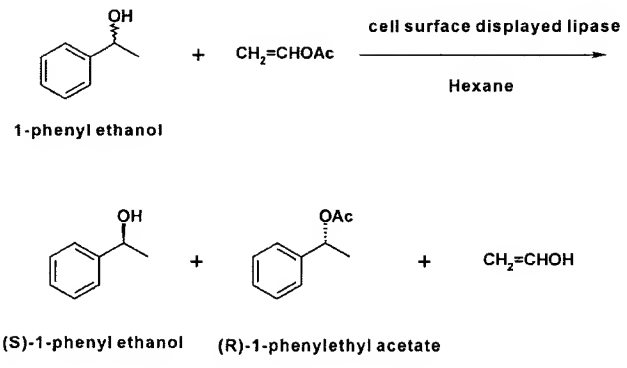

Figure 1. Reaction scheme for the enantioselective resolution of 1-phenylethanol in hexane using cell surface displayed lipase.

DNA Manipulation

Polymerase chain reaction (PCR) was performed with the PCR Thermal Cycler MP (Takara Shuzo Co., Shiga, Japan) using Expand™ High-Fidelity PCR System (Roche Molecular Biochemicals, Mannheim, Germany). DNA sequencing was carried out using the BigDye terminator cycle sequencing kit (PerkinElmer Co., Boston, MA), Taq polymerase, and ABI Prism™ 377 DNA sequencer (PerkinElmer Co.). All DNA manipulations including restriction digestion, ligation, and agarose gel electrophoresis were carried out by standard procedures (Sambrook and Russell, 2001).

Plasmids and primers used in this study are listed in Tables I and II, respectively. *P. aeruginosa oprF* and *P. fluorescens* SIK W1 lipase genes were amplified from the genomic DNA of *P. aeruginosa* and *P. fluorescens* SIK W1 using the primers designed based on the reported DNA sequences (Ahn et al., 1999; Stover et al., 2000).

Western Blotting

Proteins in the whole-cell lysates and membrane fraction were analyzed by 12% (wt/vol) SDS-PAGE. Outer membrane proteins were prepared as follows. Culture broth (3 mL) was centrifuged at 3,500*g* for 5 min at 4°C. The cell pellet was washed with 1 mL of 10 mM Na_2HPO_4 buffer (pH 7.2), centrifuged at 3,500*g* for 5 min at 4°C, and resuspended in 0.5 mL of 10 mM Na_2HPO_4 buffer (pH 7.2). Crude extracts of recombinant *E. coli* cells were prepared by three cycles of sonication (each for 20 s at 15% of maximum output; High-Intensity Ultrasonic Liquid Processors, Sonics & Material Inc., Newtown, CT). Partially disrupted cells were removed by centrifugation of sonicated samples at 12,000*g* for 2 min at room temperature. Membrane proteins and the lipid layer were isolated by centrifugation at 12,000*g* for 30 min at 4°C, followed by resuspension in 0.5 mL of 10 mM Na_2HPO_4 buffer (pH 7.2) containing 0.5% (wt/vol) sarcosyl. After incubation at 37°C for 30 min, insoluble pellet containing membrane proteins was obtained by centrifugation at 12,000*g* for 30 min at 4°C. Membrane proteins were obtained by washing the insoluble pellet with 10 mM Na_2HPO_4 buffer (pH 7.2) followed by resuspending in 50 μL of TE buffer (pH 8.0).

Western blot analysis was carried out following the standard procedure (Sambrook and Russell, 2001). For the immunodetection of the fusion protein, rat anti-lipase probe

Table I. Plasmids used in the study.

Plasmid	Relevant characteristics	Reference
pTac99A	Ap^r; *tac* promoter; 5.7 kb	Park and Lee, 2003
pTacOprF164	pTac99A derivative; containing 564-bp fragment of *oprF* of *P. aeruginosa*; 6.2 kb	This study
pTacOprF188	pTac99A derivative; containing 636-bp fragment of *oprF* of *P. aeruginosa*; 6.3 kb	This study
pTacOprF196	pTac99A derivative; containing 660-bp fragment of *oprF* of *P. aeruginosa*; 6.3 kb	This study
pTacOprF213	pTac99A derivative; containing 711-bp fragment of *oprF* of *P. aeruginosa*; 6.4 kb	This study
pTacOprF164E	pTac99A derivative; containing 564-bp fragment of *oprF* of *P. aeruginosa* and the stop codon; 6.2 kb	This study
pTacOprF188E	pTac99A derivative; containing 636-bp fragment of *oprF* of *P. aeruginosa* and the stop codon; 6.3 kb	This study
pTacOprF196E	pTac99A derivative; containing 660-bp fragment of *oprF* of *P. aeruginosa* and the stop codon; 6.3 kb	This study
pTacOprF213E	pTac99A derivative; containing 771-bp fragment of *oprF* of *P. aeruginosa* and the stop codon; 6.4 kb	This study
pTacOprF164PL	pTacOprF164 derivative; *P. fluorescens* SIK W1 lipase gene; 7.6 kb	This study
pTacOprF188PL	pTacOprF188 derivative; *P. fluorescens* SIK W1 lipase gene; 7.7 kb	This study
pTacOprF196PL	pTacOprF196 derivative; *P. fluorescens* SIK W1 lipase gene; 7.7 kb	This study
pTacOprF213PL	pTacOprF213 derivative; *P. fluorescens* SIK W1 lipase gene; 7.8 kb	This study
pTacPL	pTac99A derivative; *P. fluorescens* SIK W1 lipase gene; 7.1 kb	This study

antibodies (Peptron, Daejeon, Korea) and rabbit anti-rat immunoglobulin G (IgG)-horseradish peroxidase (HRP) conjugate (Sigma, St. Louis, MO) were used. The light-emitting nonradioactive ECL kit (Amersham Life Sciences, Buckinghamshire, U.K.) was used for signal detection.

Immunofluorescence Microscopy

For immunofluorescence microscopy, cells were harvested by centrifugation for 5 min at 3,500*g* and 4°C, washed with and resuspended in phosphate-buffered saline (PBS)

Table II. List of primers used in PCR experiments.

Primer sequence[a]	Gene to be amplified	Template
5-g**gaattc**atgaaactgaagaacaccttaggc 5-gc**tctaga**tttcgaaccaccgaagttgaag	Truncated *oprF*164	*P. aeruginosa* PAO1 chromosome
5-g**gaattc**atgaaactgaagaacaccttaggc 5[b]-gc**tctaga**ttatttcgaaccaccgaagttg	Truncated *oprF*164 with stop codon	
5-g**gaattc**atgaaactgaagaacaccttaggc 5-gc**tctaga**gacgttgtcgcaaacgccgtc	Truncated *oprF*188	*P. aeruginosa* PAO1 chromosome
5-g**gaattc**atgaaactgaagaacaccttaggc 5[b]-gc**tctaga**ttagacgttgtcgcaaacgccgtc	Truncated *oprF*188 with stop codon	
5-g**gaattc**atgaaactgaagaacaccttaggc 5-gc**tctaga**ggccggggtatccgggcactt	Truncated *oprF*196	*P. aeruginosa* PAO1 chromosome
5-g**gaattc**atgaaactgaagaacaccttaggc 5[b]-gc**tctaga**ttaggccggggtatccgggcactt	Truncated *oprF*196 with stop codon	
5-g**gaattc**atgaaactgaagaacaccttaggc 5-gc**tctaga**gcgtacgacttcggcgacagc	Truncated *oprF*213	*P. aeruginosa* PAO1 chromosome
5-g**gaattc**atgaaactgaagaacaccttaggc 5[b]-gc**tctaga**ttagcgtacgacttcggcgacagc	Truncated *oprF*213 with stop codon	
5-gc**tctaga**atgcttcatgccttcgaacgc 5-ccc**aagctt**tcaactgatcagcacacc	*P. fluorescens* SIK W1 lipase gene for fusion	*P. fluorescens* SIK W1 chromosome
5-g**gaattc**atgcttcatgccttcgaacgc 5-ccc**aagctt**tcaactgatcagcacacc	*P. fluorescens* SIK W1 lipase gene for intracellular expression	

[a]Restriction enzyme sites are shown in bold.
[b]Underlined termination sequence is added for the expression of truncated *oprF* genes.

solution supplemented with 3% (wt/vol) of bovine serum albumin (BSA, Sigma Co., St. Louis, MO). Cells were incubated with the rat anti-lipase antibodies (Peptron) diluted (1:1,000) in PBS solution containing 3 wt % BSA for 4 h. After 5 washes with PBS solution, the cell–antibody complex was incubated overnight at 4°C with rabbit anti-rat IgG conjugated with rhodamine (Santa Cruz Biotechnology, Santa Cruz, CA) at a dilution of 1:3,000. Before microscopic observation, cells were washed 5 times with PBS solution to remove unbound rabbit anti-rat IgG conjugated with rhodamine. Cells were mounted on poly-L-lysine coated microscopic slide glasses and examined by confocal microscopy (Carl Zeiss, Jena, Germany). Photographs were taken with a Carl Zeiss LSM 410 instrument.

Measurement of Enzyme Activities

Cells were harvested by centrifugation for 5 min at 5,590*g* and 4°C, washed with distilled water, and lyophilized with a TFD5505 freeze dryer (Ilshin Lab., Gyeonggi-do, Korea) for 48 h. Lipase activity was assayed by the pH-stat method (Lee et al., 1993) and the spectrophotometric method using *p*-nitrophenyl decanoate as a substrate (Lee et al., 2004b). For the latter, the activity was monitored by measuring the optical density at 405 nm using a spectrophotometer (Beckman DU650, Fullerton, CA).

The temperature-dependent lipase activities were examined using *p*-nitrophenyl decanoate as a substrate at controlled temperatures from 22 to 75°C. The optimal pH was determined at 37°C using substrate solutions having a volume ratio of 1:4:95 (10 mM *p*-nitrophenyl decanoate in acetonitrile/ethanol/50 mM potassium phosphate or 50 mM Tris-HCl at various pH values ranging from 5 to 10). For the examination of the stability of cell surface displayed lipase, 10 mg of lyophilized cells were resuspended in 10 mL of Tris-HCl (pH 8.0) and incubated at 37 or 45°C for a week. The 0.1 mL aliquots were taken, cooled to 37°C, and were added to 1 mL of substrate solution for the measurement of residual activity at 37°C for 10 min. The stability of *E. coli* cells displaying lipase in organic solvent was investigated by resuspending 10 mg of lyophilized cells in 10 mL of hexane or isopropyl alcohol, followed by 1 week of incubation at 37°C. Aliquots (0.1 mL) were removed periodically. Cells were harvested by centrifugation for 5 min at 3,500*g* and 4°C and resuspended in 1 mL of substrate solution (pH 8.0) for the measurement of residual activity at 37°C for 10 min.

Enantioselective Resolution of 1-Phenylethanol in Hexane Using *E. coli* Cells Displaying Lipase

For the enantioselective resolution, 300 mg of lyophilized cells (prepared by inducing with 0.1 mM IPTG) were resuspended in 30 mL of hexane, into which 300 mg of racemic 1-phenylethanol, 212 mg of vinyl acetate, and 3 g of 4A molecular sieves (Aldrich, St. Louis, MO) were added. The reaction mixture was incubated at 37°C and 250 rpm. Small aliquots of reaction mixture were removed during the reaction, and the products were analyzed by high-performance liquid chromatography (HPLC; Agilent 1100 HPLC system, Palo Alto, CA). Enantiomeric excess (ee) is defined as $100 \times (A - B)/(A + B)$, where A and B are the amounts of two enantiomers. The percentage of conversion is defined as $ee_s/(ee_s + ee_p)$, where subscripts s and p represent remaining substrate (alcohol) and product, respectively. The enantiomeric ratio (E) is defined as $\ln[1 - c(1 + ee_p)]/\ln[1 - c(1 - ee_p)]$ (Chen et al., 1982).

Analytical Methods

Cell growth was monitored by measuring the optical density at 600 nm, using a spectrophotometer (Beckman DU650). The yield and optical purity of chemicals were determined by HPLC equipped with a Chiralcel OB-H column (Daicel Chemical Industries, Tokyo, Japan). A mixture of hexane and isopropyl alcohol having a volume ratio of 90:10 was used as a mobile phase at a flow rate of 0.3 mL/min. Reaction products and substrates were detected by measuring absorbance at 210 nm using a diode array detector (1100 series DAD, Agilent).

RESULTS

Construction of Surface Display System

To develop a strategy for displaying the *P. fluorescens* SIK W1 lipase (49.9 kDa) using the OprF as an anchoring motif, we first searched for the potential fusion site. Based on the predicted secondary structure and information found in the literature, we chose Lys^{164}, Val^{188}, Ala^{196}, and Arg^{213} as potential fusion sites for displaying *P. fluorescens* SIK W1 lipase (Fig. 2).

The truncated *oprF* (*oprF*$_t$) genes encoding the 164, 188, 196, and 213 amino acids from the N terminus were amplified by PCR using the primer sets shown in Table II and were cloned into the *Eco*RI and *Xba*I sites of pTac99A (Park and Lee, 2003) to make pTacOprF164, pTacOprF188, pTacOprF196, and pTacOprF213, respectively. Serine and arginine were additionally inserted at the C terminus by introducing the *Xba*I site at the 3′ end of the *oprF*$_t$ gene. For the expression of the *oprF*$_t$ genes without lipase fusion, the *oprF*$_t$ genes containing the stop codon were amplified using the primer sets shown in Table II and cloned into the *Eco*RI and *Xba*I sites of pTac99A to make pTacOprF164E, pTacOprF188E, pTacOprF196E, and pTacOprF213E. The *P. fluorescens* SIK W1 lipase gene was amplified and cloned into the *Xba*I and *Hin*dIII sites of pTacOprF164, pTacOprF188, pTacOprF196, and pTacOprF213 to make pTacOprF164PL, pTacOprF188PL, pTacOprF196PL, and pTacOprF213PL, respectively, which were used for the display of lipase on the *E. coli* cell surface. For the intracellular expression of lipase as a control, the lipase gene was

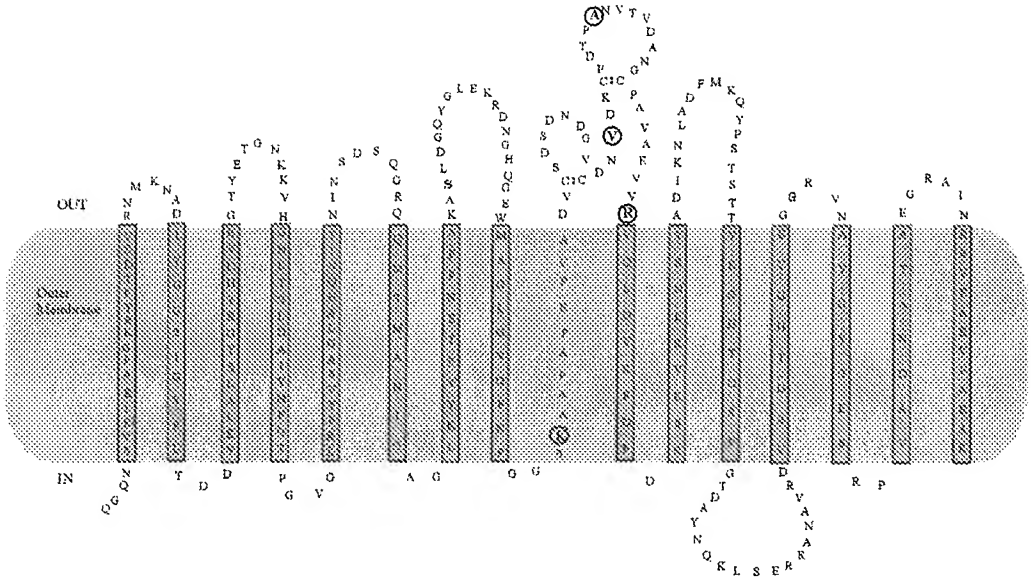

Figure 2. Proposed secondary structure of OprF redrawn from Rawling et al. (1995). Fusion sites are shown in circles.

cloned into the *Eco*RI and *Hin*dIII sites of pTac99A to make pTacPL.

Recombinant XL10-Gold cells harboring pTacOprF164PL, pTacOprF188PL, pTacOprF196PL, and pTacOprF213PL were cultivated at 37°C and induced with IPTG. Growth defects were observed for XL10-Gold cells harboring pTacOprF196PL and pTacOprF213PL. Therefore, recombinant XL10-Gold harboring pTacOprF164PL and pTacOprF188PL were used in further studies.

Confirmation of Lipase Display on the *E. coli* Cell Surface

For the confirmation of lipase display on the cell surface, the whole-cell lysates and outer membrane proteins of XL10-Gold (pTacOprF164PL) were analyzed by SDS-PAGE. Due to the low expression level, the fusion protein could hardly be detected by Coomassie blue staining (Fig. 3A). Therefore, western blot analysis was carried out using the rat anti-lipase antibody which was subsequently detected with HRP-conjugated rabbit anti-rat IgG (Fig. 3B). Signal was not detected in whole-cell lysates of *E. coli* XL10-Gold (pTacOprF164E) producing $OprF_t$ protein (Fig. 3B, lane 1). The bands corresponding to approximately 68-kDa fusion protein were detected in whole-cell lysates and outer membrane fraction (Fig. 3B, lanes 2 and 3), suggesting a successful display of lipases on the cell surface.

The display of lipase on the *E. coli* cell surface could also be directly confirmed by immunofluorescence microscopy. As shown in Figure 4, *E. coli* XL10-Gold (pTacOprF164PL) producing fusion protein became fluorescent due to the binding of anti-lipase antibody followed by binding of rhodamine-conjugated secondary antibody, indicating that lipase was successfully displayed on the surface of *E. coli* (Fig. 4C). On the other hand, *E. coli* XL10-Gold cells harboring pTacOprF164E or pTacPL were not fluorescent at all (Fig. 4A,B).

After confirming that lipases were successfully displayed on the *E. coli* cell surface, we examined if the displayed lipases were active. By the pH-stat method, the whole-cell lipase activities of 1,290 ± 96.1 and 932 ± 82 U/g lyophilized cell were obtained for XL10-Gold harboring pTacOprF164PL and pTacOprF188PL, respectively, which were induced with 0.1 mM IPTG. On the other hand, the lipase activity of supernatant was negligible in all cases, suggesting that cell lysis was not a problem. These results suggest that lipases were successfully displayed in an active form using the $OprF_t$ as an anchoring motif. For comparison, the activity of lipase produced intracellularly was also measured. The whole-cell activity of XL10-Gold (pTacPL) induced with 0.1 mM IPTG was 235 ± 48 U/g

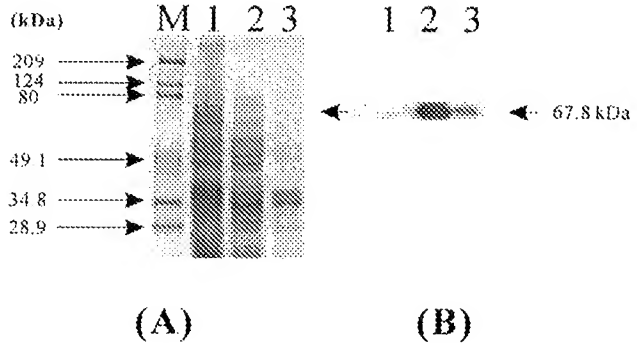

Figure 3. SDS-PAGE analysis (**A**) and immunoblotting (**B**) of *E. coli* XL10-Gold expressing $OprF_t$ and $OprF_t$–lipase fusion protein: molecular weight standards (lane M), whole-cell lysates of *E. coli* XL10-Gold harboring pTacOprF164E (lane 1), whole-cell lysates of *E. coli* XL10-Gold harboring pTacOprF164PL (lane 2), and outer membrane fraction of *E. coli* XL10-Gold harboring pTacOprF164PL (lane 3).

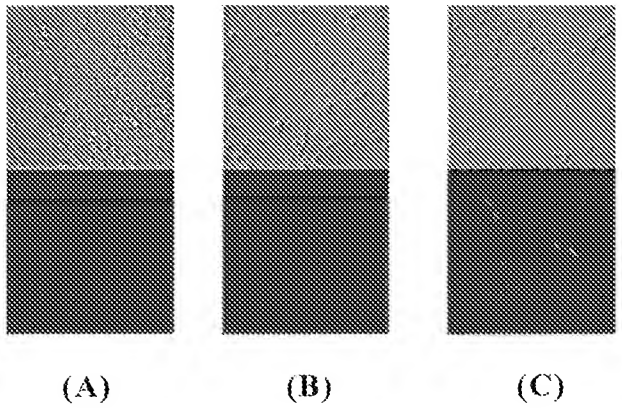

Figure 4. Differential interference micrographs (upper) and immunofluorescence micrographs (lower) of recombinant *E. coli* XL10-Gold harboring pTacPL (**A**), pTacOprF164E (**B**), and pTacOprF164PL (**C**). Cells were incubated with rat anti-lipase probe antibody followed by probing with rabbit anti-rat IgG-rhodamine conjugate. Fluorescence is seen only in (**C**).

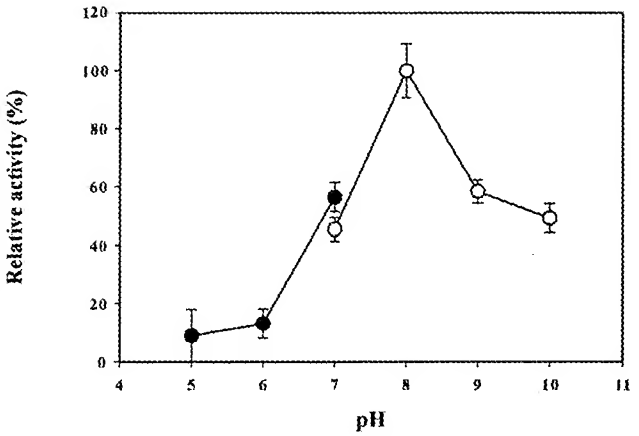

Figure 6. Effect of pH on the lipase activity of surface displayed lipase. The enzyme activity was determined at 37°C using *p*-nitrophenyl decanoate as a substrate. Relative activity was calculated by assuming the activity obtained at pH 8.0 as 100%. Buffers used were 50 mM potassium phosphate buffer (●) and 50 mM Tris-HCl (○).

lyophilized cell, which was much lower than that obtained with cell surface displayed lipase. When the cells were induced with 1 mM IPTG, cell surface displayed lipase (XL10-Gold harboring pTacOprF164PL) and intracellularly expressed lipase showed much lower activities of 350 ± 57 U/g lyophilized cell and 194 ± 41 U/g lyophilized cell, respectively.

Activity and Stability of Cell Surface Displayed Lipase

To determine the enzymatic characteristics of cell surface displayed lipase, whole-cell lipase activities of lyophilized XL10-Gold harboring pTacOprF164PL were measured at various temperatures ranging from 22 to 75°C and pH values ranging from 5 to 10. The results are shown in Figures 5 and 6. Cell surface displayed lipase showed the maximum activity at 37°C and pH 8.0. In the temperature range of 37 to 45°C, the whole-cell activities were maintained higher than 90% of the maximum activity. After the optimization of reaction condition, the enzyme stability against heat and different solvents was examined because it is important for industrial applications. Cell surface displayed lipase was incubated at 37°C in Tris-HCl, isopropyl alcohol, and hexane for a week, during which the whole-cell lipase activity was measured periodically. As shown in Figure 7, the cell surface displayed lipase was quite stable and retained 80% of the initial activity (Fig. 7) in all solvents during the entire reaction time. The lipase activity of supernatant was negligible throughout the entire reaction, suggesting that cells were not lysed. All these

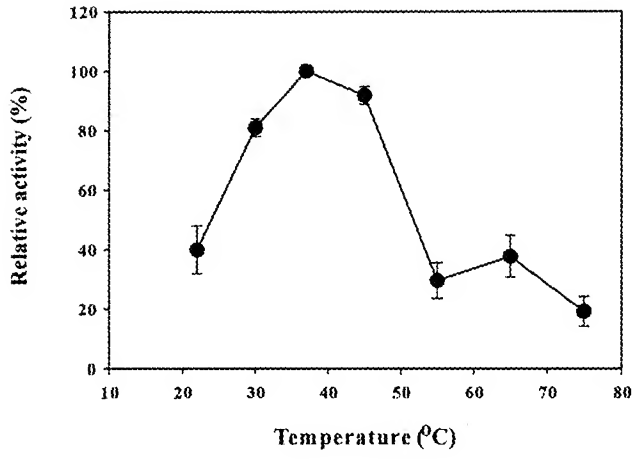

Figure 5. Effect of temperature on the activity of surface displayed lipase. The enzyme activity was determined at pH 8.0 using *p*-nitrophenyl decanoate as a substrate. Relative activity was calculated by assuming the activity obtained at 37°C as 100%.

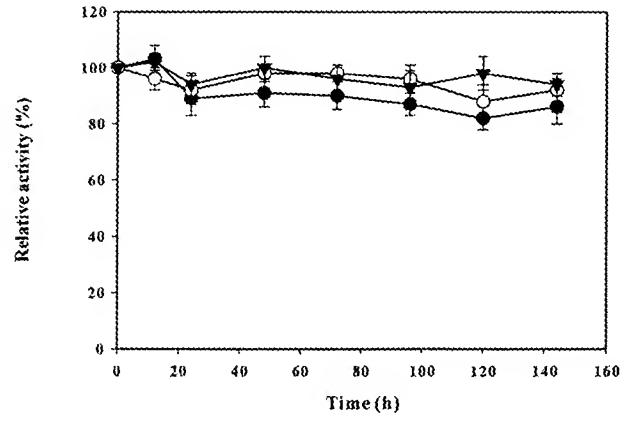

Figure 7. Stability of lipase displayed on the cell surface of *E. coli* XL10-Gold (pTacOprF164PL) during the prolonged incubation at 37°C. Cells were incubated in Tris-HCl pH 8.0 (●), isopropyl alcohol (○), and hexane (▼). The enzyme activity was determined at 37°C and pH 8.0 using *p*-nitrophenyl decanoate as a substrate. Relative activity was calculated by assuming the initial activity as 100%.

results suggest that *E. coli* cells displaying lipase can be used as an efficient biocatalyst.

Enantioselective Resolution of 1-Phenylethanol Using Cell Surface Displayed Lipase

As one of the important biocatalytic applications, we investigated the enantioselective resolution of a racemic compound using cell surface displayed lipase in organic solvent using 1-phenylethanol as a substrate (Fig. 1). After 36 h, the enantiomeric excesses of remaining 1-phenylethanol and product (*R*)-phenyl ethyl acetate were 32% and 96.3%, respectively. The percentage of conversion was 25% with an enantiomeric ratio of 74.8. These results suggest that cell surface displayed lipase using $OprF_t$ anchor has potentials for the enantioselective reaction in organic solvents.

DISCUSSION

Even though microbial cell surface display has a great potential to be used in a wide range of applications, it has found only limited applications due to the limited availability of optimized anchoring motifs to efficiently display proteins having different molecular weights and molecular characteristics. The anchoring motif, which is quite successful in displaying some target proteins, often fails to display other proteins. Therefore, development of a successful cell surface display system depends on finding an optimized anchoring motif suitable for target proteins desired. Using different surface anchoring motifs, several enzymes including levansucrase, organophosphorus hydrolase, lipase, dimeric bovine adrenodoxin, and carboxymethylcellulase have been displayed on the cell surface (Jose et al., 2002; Jung et al., 1998, 2003; Lee et al., 2003; Matsumoto et al. 2002; Shimazu et al., 2001).

In this study, we developed a cell surface display system using the *P. aeruginosa* outer membrane protein OprF as an anchoring motif via C-terminal deletion–fusion strategy. This strategy allowed successful display of lipase in an active form on the surface of *E. coli*. Previously, Val^{188}, Ala^{196}, and Arg^{213} of OprF were suggested to be possible fusion sites for the display of small peptides (Wong et al., 1995). However, Ala^{196} and Arg^{213} were found to be not suitable for larger protein display because cells did not grow well after over-expression of fusion protein. This is likely due to the membrane instability observed frequently during cell surface display (Shimazu et al., 2001). However, we do not know the exact mechanism behind this. Nonetheless, Val^{188} was found to be a suitable fusion site for the display of lipase. Rawling et al. (1998) reported that the amino acids 154 to 163 from the N-terminus are essential for the stable production of OprF. Therefore, we examined Lys^{164} as another potential fusion site. XL10-Gold harboring pTacOprF164PL showed the highest whole-cell lipase activity, suggesting that Lys^{164} is the best site for fusing the lipase among those tested.

The number of lipase molecules displayed per cell was estimated next. It was assumed that the displayed lipase would have the same specific activity of the purified enzyme (12,918 U/mg protein; Lee and Rhee, 1996). It was further assumed that 1 mg of lipase (49.9 kDa) corresponds to 1.2×10^{16} molecules and 1 g of lyophilized cell corresponds to 3.6×10^{12} cells. Then recombinant *E. coli* XL10-Gold (pTacOprF164PL) having the specific activity of 1,290 U/g lyophilized cell would have 333 lipase molecules displayed per cell. This is more than that obtained with the OmpC anchoring system (294 molecules per cells; Lee et al., 2004a). Furthermore, lipase displayed in this manner showed good enzymatic characteristics (Figs. 5–7). This good enzyme stability is one of the most important features for industrial biocatalytic processes. It is notable that lipase displayed using $OprF_t$ (164 amino acids) as an anchoring motif showed excellent stability. Lyophilized cells displaying lipase were stable in both aqueous solution and organic solvents. In addition, recombinant *E. coli* cells displaying lipases did not show any growth defects. Matsumoto et al. (2004) reported that yeast surface displayed lipases were highly active and stable in several organic solvents during relative short reaction time (60 h). Recombinant *E. coli* displaying lipase using the OprF anchoring system was a little less active than the yeast system but much more stable after prolonged incubation (7 days) in organic solvent.

It has been reported that lipase can be displayed on the cell surface of several microorganisms (Kobayashi et al., 2002; Jung et al., 2003; Lee et al., 2004a, 2004b; Matsumoto et al., 2004; Samuelson et al., 1999). However, the yeast display system has been the only one that was used for enantioselective resolution of racemic compounds in organic solvent. Recombinant *E. coli* displaying lipase on the cell surface was also able to carry out enantioselective resolution of racemic compound in organic solvent. During the reaction at 37°C in hexane, cell lysis was negligible. It should be noted that recombinant *E. coli* displaying lipases allowed higher enantiomeric ratio and higher enantiomeric excess than those typically obtainable by using the free lipase system (Cardenas et al., 2001). When molecular sieves were not included in the reaction, little transesterification occurred (data not shown). It has been known that the excess content of water can inhibit lipase-catalyzed transesterification (Kyotani et al., 1988; Matsumoto et al., 2004). This was also true for recombinant *E. coli* displaying lipase as removal of excess water by adding molecular sieves was necessary for enantioselective transesterification reaction.

In conclusion, we have shown that the C-terminal deletion–fusion of lipase to the OprF anchor allowed successful display of lipase on the *E. coli* cell surface. We also demonstrated for the first time that *E. coli* cells display lipases could catalyze enantioselective resolution in organic solvent with high stability, suggesting that it can be used as a cost-effective biocatalytic system for various biotechnological applications.

We thank Prof. J.S. Rhee and Dr. J.K. Song at KAIST for kindly providing the *P. fluorescens* SIK W1 strain and helpful discussions. Support by the LG Chem Chair professorship, IBM SUR program, BK21 project, and the Center for Ultramicrochemical Process Systems are appreciated.

References

Adam W, Groer P, Humpf HU, Saha-Möller CR. 2000. Synthesis of optically active α-methylene β-lactams through lipase-catalyzed kinetic resolution. J Org Chem 65:4919–4922.

Ahn JH, Pan JG, Rhee JS. 1999. Identification of the *tliDEF* ABC transporter specific for lipase in *Pseudomonas fluorescens* SIK W1. J Bacteriol 181:1847–1852.

Benhar I. 2001. Biotechnological applications of phage and cell display. Biotechnol Adv 19:1–33.

Burton SG, Cowan DA, Woodley JM. 2002. The search for the ideal biocatalyst. Nat Biotechnol 20:37–45.

Cardenas F, de Castro MS, Sanchez-Montero JM, Sinisterra JV, Valmaseda M, Elson SW, Alvarez E. 2001. Novel microbial lipases: catalytic activity in reactions in organic media. Enzyme Microb Technol 28:145–154.

Chen CS, Fujimoto Y, Girdaukas G, Sih CJ. 1982. Quantitative analyses of biochemical kinetic resolutions of enantiomers. J Am Chem Soc 104: 7294–7299.

Drauz K, Waldmann H. 2002. Enzyme catalysis in organic synthesis: a comprehensive handbook, 2nd edition. Weinheim, Germany: Wiley-VCH Verlag GmbH. 1559 p.

Georgiou G, Stathopoulos C, Daugherty PS, Nayak AR, Iverson BL, Curtiss RI. 1997. Display of heterologous proteins on the surface of microorganisms: from the screening of combinatorial libraries to live recombinant vaccines. Nat Biotechnol 15:29–34.

Jaeger KE, Dijkstra BW, Reetz MT. 1999. Bacterial biocatalysts: molecular biology, Three-dimensional structures, and biotechnological applications of lipase. Annu Rev Microbiol 53:315–351.

Jose J, Bernhardt R, Hannemann F. 2002. Cellular surface display of dimeric Adx and whole cell P_{450}-mediated steroid synthesis on *E. coli*. J Biotechnol 95:257–268.

Jung HC, Ko S, Ju SJ, Kim EJ, Kim MK, Pan JG. 2003. Bacterial cell surface display of lipase and its randomly mutated library facilitates high-throughput screening of mutants showing higher specific activities. J Mol Catal B 26:177–184.

Jung HC, Lebeault JM, Pan JG. 1998. Surface display of *Zymomonas mobilis* levansucrase by using the ice-nucleation protein of *Pseudomonas syringae*. Nat Biotechnol 16:576–580.

Koeller KM, Wong CH. 2001. Enzymes for chemical synthesis. Nature 409:232–240.

Kyotani S, Fukuda H, Morikawa H, Yamane T. 1988. Interesterification of fats and oils by immobilized fungus at constant water concentration. J Ferment Technol 66:71–83.

Kobayashi G, Fujii K, Serizawa M, Yamamoto H, Sekiguchi J. 2002. Simultaneous display of bacterial and fungal lipases on the cell surface of *Bacillus subtilis*. J Biosci Bioeng 93:15–19.

Lalonde JJ, Navia MA, Margolin AL. 1997. Cross-linked enzyme crystals of lipases as catalysts for kinetic resolution of acids and alcohols. Methods Enzymol 286:443–464.

Lee SH, Choi JH, Park SH, Choi J-I, Lee SY. 2004a. Enantioselective resolution of racemic compounds by cell surface displayed lipase. Enzyme Microbial Technol 35:429–436.

Lee SH, Choi J-I, Park SJ, Lee SY, Park BC. 2004b. Display of bacterial lipase on the *Escherichia coli* cell surface by using FadL as an anchoring motif and its use in enantioselective biocatalysis. Appl Environ Microbiol 70:5074–5080.

Lee SY, Choi JH, Xu J. 2003. Microbial cell surface display. Trends Biotechnol 21:45–52.

Lee YP, Chung GH, Rhee JS. 1993. Purification and characterization of *Pseudomonas fluorescens* SIK W1 lipase expressed in *Escherichia coli*. Biochim Biophys Acta 1169:156–164.

Lee YP, Rhee JS. 1996. Protein aggregation and adsorption upon in vitro refolding of recombinant *Pseudomonas* lipase. J Microbiol Biotechnol 6:456–460.

Matsumoto T, Fukuda H, Ueda M, Tanaka A, Kondo A. 2002. Construction of yeast strains with high cell surface lipase activity by using novel display systems based on the Flo1p flocculation functional domain. Appl Environ Microbiol 68:4517–4522.

Matsumoto T, Ito M, Fukuda H, Kondo A. 2004. Enantioselective transesterification using lipase-displaying yeast whole-cell biocatalyst. Appl Microbiol Biotechnol 64:481–485.

Nikaido H, Nikaido K, Harayama S. 1991. Identification and characterization of porins in *Pseudomonas aeruginosa*. J Biol Chem 266: 770–779.

Pàmies O, Bäckvall JE. 2002. Enzymatic kinetic resolution and chemoenzymatic dynamic kinetic resolution of δ-hydroxy esters. An efficient route to chiral δ-lactones. J Org Chem 67:1261–1265.

Park SJ, Lee SY. 2003. Identification and characterization of a new enoyl coenzyme A hydratase involved in biosynthesis of medium-chain-length polyhydrolxyalkanoates in recombinant *Escherichia coli*. J Bacteriol 185:5391–5397.

Patel RN. 2000. Stereoselective biocatalysis. New York: Marcel Dekker. 932 p.

Rawling EG, Brinkman FSL, Hancock REW. 1998. Roles of the carboxy-terminal half of *Pseudomonas aeruginosa* major outer membrane protein OprF in cell shape, growth in low-osmolarity medium, and peptidoglycan association. J Bacteriol 180:3556–3562.

Rawling EG, Martin NL, Hancock REW. 1995. Epitope mapping of the *Pseudomonas aeruginosa* major outer membrane porin protein OprF. Infect Immun 63:38–42.

Sambrook J, Russell DW. 2001. Molecular cloning: a laboratory manual, 3rd edition. Plainview, NY: Cold Spring Harbor Laboratory Press.

Samuelson P, Cano F, Robert A, Ståhl S. 1999. Engineering of a *Staphylococcus carnosus* surface display system by substitution or deletion of a *Staphylococcus hyicus* lipase propeptide. FEMS Lett 179:131–139.

Samuelson P, Gunneriusson E, Nygren PA, Ståhl S. 2002. Display of proteins on bacteria. J Biotechnol 96:129–154.

Schöfer SH, Kaftzik N, Wasserscheid P, Kragl U. 2001. Enzyme catalysis in ionic liquids: lipase-catalysed kinetic resolution of 1-phenylethanol with improved enantioselectivity. Chem Commun 425–426.

Sharfuddin M, Narumi A, Iwai Y, Miyazawa K, Yamada S, Kakuchic T, Kaga H. 2003. Lipase-catalyzed dynamic kinetic resolution of hemiaminals. Tetrahedron: Asymmetry 14:1581–1585.

Shimazu M, Mulchandani A, Chen W. 2001. Cell surface display of organophosphorus hydrolase using ice nucleation protein. Biotechnol Prog 17:76–80.

Stover CK, Pham XQT, Erwin AL, Mizoguchi SD, Warrener P, Hickey MJ, Brinkman FSL, Hufnagle WO, Kowalik DJ, Lagrou M, Garber RL, Goltry L, Tolentino E, Westbrock-Wadman S, Yuan Y, Brody LL, Coulter SN, Folger KR, Kas A, Larbig K, Lim RM, Smith KA, Spencer DH, Wong GKS, Wu Z, Paulsen IT, Reizer J, Saier MH, Hancock REW, Lory S, Olson MV. 2000. Complete genome sequence of *Pseudomonas aeruginosa* PA01, an opportunistic pathogen. Nature 406:959–964.

Wittrup KD. 2001. Protein engineering by cell-surface display. Curr Opin Biotechnol 12:395–399.

Wong RSY, Wirtz RA, Hancock REW. 1995. *Pseudomonas aeruginosa* outer membrane protein OprF as an expression vector for foreign epitopes: the effects of positioning and length on the antigenicity of the epitope. Gene 158:55–60.

Woodruff WA, Parr TR Jr, Hancock RE, Hanne LF, Nicas TI, Iglewski BH. 1986. Expression in *Escherichia coli* and function of *Pseudomonas aeruginosa* outer membrane porin protein F. J Bacteriol 167:473–479.

Xu Z, Lee SY. 1999. Display of polyhistidine peptides on the *Escherichia coli* cell surface by using outer membrane protein C as an anchoring motif. Appl Environ Microbiol 65:5142–5147.